doi:10.1093/brain/awt083 Brain 2013: 136; 1415–1431 | 1415

BRAIN
A JOURNAL OF NEUROLOGY

Reactive glia show increased immunoproteasome activity in Alzheimer's disease

Marie Orre,[1,$] Willem Kamphuis,[1,$] Stephanie Dooves,[1,*] Lieneke Kooijman,[1] Elena T. Chan,[2] Christopher J. Kirk,[2] Vanessa Dimayuga Smith,[1,#] Sanne Koot,[1] Carlyn Mamber,[1] Anne H. Jansen,[1,&] Huib Ovaa[3] and Elly M. Hol[1,4]

1 Astrocyte Biology and Neurodegeneration, Netherlands Institute for Neuroscience (NIN), an Institute of the Royal Netherlands Academy of Arts and Sciences, Amsterdam, The Netherlands
2 Onyx Pharmaceuticals, South San Francisco, USA
3 Division of Cell Biology, Netherlands Cancer Institute, Amsterdam, The Netherlands
4 Swammerdam Institute for Life Sciences, Centre for Neuroscience, University of Amsterdam, The Netherlands

[$]These authors contributed equally to this work.
*Present address: Department of Child Neurology, VU University Medical Centre, Amsterdam, The Netherlands
[#]Present address: Mayo Clinic College of Medicine, Rochester, Minnesota, USA
[&]Present address: Department of Cell Biology and Histology, Academic Medical Centre, University of Amsterdam, Amsterdam, The Netherlands

Correspondence to: Elly M. Hol
Meibergdreef 47,
1105 BA, Amsterdam,
The Netherlands
E-mail: e.hol@nin.knaw.nl

The proteasome is the major protein degradation system within the cell, comprised of different proteolytic subunits; amyloid-β is thought to impair its activity in Alzheimer's disease. Neuroinflammation is a prominent hallmark of Alzheimer's disease, which may implicate an activation of the immunoproteasome, a specific proteasome variant induced by immune signalling that holds slightly different proteolytic properties than the constitutive proteasome. Using a novel cell-permeable proteasome activity probe, we found that amyloid-β enhances proteasome activity in glial and neuronal cultures. Additionally, using a subunit-specific proteasome activity assay we showed that in the cortex of the APPswePS1dE9 plaque pathology mouse model, immunoproteasome activities were strongly increased together with increased messenger RNA and protein expression in reactive glia surrounding plaques. Importantly, this elevated activity was confirmed in human post-mortem tissue from donors with Alzheimer's disease. These findings are in contrast with earlier studies, which reported impairment of proteasome activity in human Alzheimer's disease tissue and mouse models. Targeting the increased immunoproteasome activity with a specific inhibitor resulted in a decreased expression of inflammatory markers in *ex vivo* microglia. This may serve as a potential novel approach to modulate sustained neuroinflammation and glial dysfunction associated with Alzheimer's disease.

Keywords: Alzheimer's disease; immunoproteasome; neuroinflammation; microglia; astrocytes
Abbreviation: AMC = 7-amino-4-methylcoumarin

Received August 30, 2012. Revised January 21, 2013. Accepted February 11, 2013
© The Author (2013). Published by Oxford University Press on behalf of the Guarantors of Brain. All rights reserved.
For Permissions, please email: journals.permissions@oup.com

Downloaded from https://academic.oup.com/brain/article/136/5/1415/287013 by guest on 16 August 2022

Introduction

One of the major hallmarks of Alzheimer's disease is the deposition of extracellular plaques, composed of aggregated amyloid-β. Other hallmarks of Alzheimer's disease are the presence of intraneuronal aggregates of hyperphosphorylated tau (Selkoe, 2001), activated microglia (Perry *et al*., 2010), and astrogliosis (Beach *et al*., 1989). An accumulation of aberrant and ubiquitinated proteins in association with amyloid-β plaques, tangles and dystrophic neurites is observed in Alzheimer's disease brains, and has been postulated to be the result of an impaired ubiquitin proteasome system (De Vrij *et al*., 2004). The ubiquitin proteasome system is the main protein degradation system within cells; it plays a key role in degrading aberrant proteins and is involved in a variety of vital cellular processes, such as degrading short-lived proteins, and generation of peptides for antigen presentation on Major Histocompatibility Complex class I molecules. The proteolytic component of the ubiquitin proteasome system is the proteasome. The constitutive proteasome is composed of a 20S core including three proteolytic subunits, β1, β2 and β5, each possessing a different enzymatic activity; caspase-like, trypsin-like and chymotrypsin-like, respectively (Goldberg, 2003; De Vrij *et al*., 2004). Pro-inflammatory mediators, such as interferon gamma (IFNγ), induce the formation of a proteasome variant termed the immunoproteasome. The immunoproteasome has distinct proteolytic subunits (β1i, β2i and β5i) making it better equipped for cleavage of peptides for antigen presentation, which is believed to be its main function (Früh *et al*., 1994; Kincaid *et al*., 2011). Recent studies show that the immunoproteasome also has immune regulatory functions, involved in the modulation of innate immune signalling (Groettrup *et al*., 2010).

Several studies have provided evidence for an impaired proteasome activity in Alzheimer's disease but these assays did not discriminate between immunoproteasome and constitutive proteasome-mediated activities. Assays in homogenates from Alzheimer's disease affected brain areas showed impaired chymotrypsin-like and caspase-like proteasome activities (Keller *et al*., 2000; Keck *et al*., 2003; Mishto *et al*., 2006). Inhibition of proteasome activity has also been shown in several Alzheimer's disease mouse models (Oh *et al*., 2005; Almeida *et al*., 2006; Tseng *et al*., 2008). However, there are also data providing evidence that Alzheimer's disease is linked to an increased proteasome activity. Cell lysates of amyloid-β treated primary rat astrocytes showed an initial impairment of chymotrypsin-like activity, followed by an increase at later time points (Schubert *et al*., 2009). Increased immunoproteasome activity may also be expected as a result of the plaque-related inflammatory signalling in Alzheimer's disease (Palombella *et al*., 1994; Hickman *et al*., 2008; Kamphuis *et al*., 2012). Moreover, our group has previously found that inhibition of the proteasome leads to a decrease in expression of the astrocyte reactivity markers, glial fibrillary acidic protein (GFAP) and vimentin (Middeldorp *et al*., 2009). This is in sharp contrast with the high levels of GFAP expression in reactive astrocytes surrounding plaques (Beach *et al*., 1989; Kamphuis *et al*., 2012). We concluded that the evidence for a decreased proteasome activity in Alzheimer's disease tissue presented so far is not entirely conclusive and that an increased proteasome would actually be more in line with our expectation. Studies to date have mainly focused on the effect of amyloid-β on proteasome activity in neurons. However, reactive astrocytes and activated microglia in the inflammatory environment in Alzheimer's disease brains may respond differently to extracellular amyloid-β and plaques. Here, we studied the effects of amyloid-β on proteasome activity on different cell types *in vitro* and the alterations of proteasome in a mouse model for Alzheimer's disease and in post-mortem human Alzheimer's disease tissue.

Materials and methods

Cell culture, treatment and differentiation

Mouse astrocytoma Ink/Arf$^{-/-}$ cells were cultured in Dulbecco's modified Eagle's medium/F-12 medium supplemented with 10% foetal bovine serum and 1% penicillin/streptomycin; the mouse immortalized microglia N9 were cultured in Dulbecco's modified Eagle's medium glutamax and 5% foetal bovine serum, 1% penicillin/streptomycin and 1% sodium pyruvate; and the mouse neuroblastoma cell line N2A was cultured in Dulbecco's modified Eagle's medium GlutaMAX^{TM} and 10% foetal bovine serum, 1% penicillin/streptomycin and differentiated by serum starvation (0.5% foetal bovine serum) for 3 days. All cells were kept in a 37°C/5% CO2 incubator. Cells were treated with amyloid-β_{1-42} fibrils or oligomers 1.0 μM, 0.1 μM. For proteasome inhibition a dilution series of Epoxomicin (Santa Cruz Biotechnology) was used. All culture media were purchased from Invitrogen. Primary cells used for amyloid-β treatment were isolated as described previously (Mamber *et al*., 2012) from p3 mouse cortex. After dissociation, cells were allowed to adhere to the uncoated plastic bottom of a cell culture flask, after 2 h the supernatant was removed, adherent cells containing a mix of astrocytes and microglia were allowed to grow for 14 days prior to usage for amyloid-β treatment.

Mice

APPswePS1dE9 double-transgenic mice (Alzheimer's disease) (Jankowsky *et al*., 2004) were studied. For analysis of ubiquitin proteasome system functioning *in vivo*, the UbG76VGFP/2 mice (Lindsten *et al*., 2003) were crossed with the APPswePS1dE9 mice to generate Alzheimer's disease mice with a green fluorescent protein (GFP) ubiquitin proteasome system reporter. All animals were housed under standard conditions. Experimental procedures were approved by the ethical committee for animal care and use of the Royal Netherlands Academy of Arts and Sciences.

For immunofluorescence, groups of animals were studied at the age of 3, 6, 9, 12, 15 and 18 months. Each age group was composed of Alzheimer's disease-wild-type littermate pairs that were sex-matched. For quantitative PCR assays, RNA isolated from the cortex of 5–8 animals with Alzheimer's disease was compared with RNA isolated from 8–11 wild-type mice of the same age groups. For proteasome activity assays, frozen cortices from the same mice were used. For the quantitative PCR, immunohistochemistry, and proteasome activity experiments equal numbers of male and female mice

Downloaded from https://academic.oup.com/brain/article/136/5/1415/287013 by guest on 16 August 2022

were used. As no significant differences were noted, males and females were pooled.

Immunofluorescence and immunohistochemical procedures

Coronal cryosections (10 μm) of mouse cortical tissue and human post-mortem hippocampal/entorhinal cortex tissue were post-fixed in 4% paraformaldehyde in PBS, pH 7.0, at room temperature. Sections were blocked with 0.05 M phosphate buffer supplemented with 10% normal donkey serum and 0.4% Triton™ X-100, incubated overnight with the primary antibodies diluted in 3% normal donkey serum and 0.4% Triton™ X-100 in phosphate buffer at room temperature. For antibodies see Supplementary Table 2. Negative controls were included by omitting the primary antibody, but these never yielded staining patterns. For mouse tissue, fluorescence visualization was used with Cy3- or Alexa Fluor® 488-conjugated secondary antibodies. Sections were washed and cover-slipped in Vectashield, including DAPI as a nuclear dye (Vector Laboratories) and viewed with a Leica DMRE fluorescence microscope. For immunohistochemistry on human tissue, 3,3′-diaminobenzidine (DAB) and alkaline phosphatase double staining was done using biotinylated- and alkaline phosphatase-labelled secondary antibodies. Before DAB development, an amplification step was performed, using avidin-biotin complex (1:800 in phosphate buffer; Vector laboratories), followed by washing and incubation with DAB solution (Sigma-Aldrich). For development of alkaline phosphatise, the Vector® Blue Substrate Kit (Vector laboratories) was used according to manufacturers' instructions. Images of DAB/alkaline phosphatase double labelling with pseudocolours were taken on an AxioVert microscope with Neoplanfluor objectives using the multispectral imaging system camera CRI Nuance FX (Quorum Technologies Inc) and the Nuance software (Cambridge Research and Instrumentation inc). Immunohistochemistry was performed on tissue from four different donors. Adobe Photoshop was used to arrange the TIFF files for presentation. For quantification of the BrdU/β5i co-localization and Iba1 stain in the mouse tissue, cell counts were made bilaterally in the neocortex. The cell counts were averaged reflecting the number of cells observed in a single 10 μm section per unilateral side (hemisphere), $n = 4–6$ mice as in Kamphuis *et al*. (2012).

Amyloid-β peptide preparations

Preparation of oligomeric amyloid-β and fibrillar amyloid-β was done as described previously (Chafekar *et al*., 2007). Amyloid-$\beta_{1–42}$ peptides (Anaspec) were dissolved in HFIP (1,1,1,3,3,3-hexafluoroisopropanol) (Sigma) at a final concentration of 1 mg/ml, followed by SpeedVac®. The peptide film was dissolved in dimethyl sulphoxide and sonicated. For amyloid-$\beta_{1–42}$ oligomers, the peptide/dimethyl sulphoxide mix was added to ice-cold 25 mM PBS, pH 7.4 during vortexing, followed by incubation at 4°C for 24 h, followed by centrifugation. The supernatant containing the oligomeric fraction was snap frozen and stored at -80°C. For amyloid-$\beta_{1–42}$ fibrils; the peptide/dimethyl sulphoxide mixture was added to 10 mM HCl, vortexed, incubated at 37°C for 48 h, and centrifuged. The pellet containing the fibrils was dissolved in 10 mM HCl/5% dimethyl sulphoxide, snap frozen, and stored at –80°C. Beta sheet content was measured by thioflavin T assay (Sigma) and protein concentrations by Bradford (Bio-Rad) according to manufacturer's protocol. Aggregation was checked on western blot using 12% Bis/Tris gels (Invitrogen) blotted on nitrocellulose membrane and stained with 6E10 antibody.

Proteasome activity in living cells

Cell lines were treated with amyloid-$\beta_{1–42}$ fibrils or oligomers at concentrations of 0.1 μM or 1.0 μM for 72 h. After washing in foetal bovine serum-free Dulbecco's modified Eagle's medium, the cells were incubated with 200 nM Bodipy-tagged, cell-permeable, proteasome activity probe, BodipyFL-Ahx3L3VS (Berkers *et al*., 2007) for 2 h. Cells were trypsinized and washed in Dulbecco's modified Eagle's medium followed by centrifugation at 200*g*, 5 min at 4°C and resuspended in PBS/1% bovine serum albumin, 7AAD (BD biosciences) viability dye was added, followed by analysis by flow cytometer using a BD FACS Calibur (BD Biosciences). For cell lines, the geometric mean of probe intensity from 20 000 viable cells was used as measurement for average sample proteasome activity. A co-culture of primary astrocytes and microglia were treated with 1.0 μM oligomeric amyloid-β or fibrillar amyloid-β for 72 h and analysed using the proteasome probe as described above. The microglia were labelled with an APC conjugated anti-CD11b antibody (eBioscience), which enabled us to separate astrocytes from microglia by flow cytometric analysis. A total of 6000–20 000 primary glia cells were analysed per condition. The geometric mean of the probe intensity was assessed in the CD11b+ microglia and the CD11b− astrocytes separately. For all cell types and cell lines, amyloid-β-treated samples were compared with mock treated control samples in each assay.

Tissue and cell homogenization

Tissue

Snap frozen left cortices from APPswePS1dE9 mice and wild-type littermates were homogenized in a pair-wise manner in homogenization buffer (50 mM HEPES, 250 mM sucrose, 5 mM $MgCl_2$, 0.5 mM DTT and 40 mM KCl pH 7.4). Homogenates were prepared using an ultra turrax, followed by centrifugation at 4°C as follows: 1300*g* for 10 min; 10 000*g* for 10 min and 13 000*g* for 25 min, transferring the supernatant in each step. The protein concentration of the final supernatant was determined with the BCA protein assay kit (Thermo Fisher) by using a fluormetric 96-well reader (Varioskan Flash reader, Thermo Fisher Scientific).

Cells

Cells were cultured in 6-well plates and treated with amyloid-$\beta_{1–42}$ oligomers or fibrils at concentrations of 0.1 μM, 1.0 μM or mock as control for 72 h. Cells were trypsinized, washed, and pelleted at 200*g*, 5 min at 4°C. The pellets were resuspended in 200 μl homogenization buffer and incubated with Digitonin 0.025% (Invitrogen) on ice for 5 min. The cytosolic cell fraction was 'squeezed out' by centrifugation at 20 000*g* for 15 min at 4°C. The cytosolic protein content was measured by Bradford assay and 20 μg of protein was used for analysis of proteasome activity using 7-amino-4-methyl coumarine (AMC) conjugated reported peptides.

Proteasome activity assay in brain homogenates using AMC conjugated peptides

The AMC conjugated activity-specific peptides were used to assess the different proteasome subunit activities, 50 μM Boc-LRR-AMC for the trypsin-like activity, 50 μM Suc-LLVY-AMC for chymotrypsin-like activity (both BostonBiochem), and 25 μM Ac-nLPnLD-AMC (Bachem AG) to measure the caspase-like activity. Protein (20 μg per reaction)

Downloaded from https://academic.oup.com/brain/article/136/5/1415/287013 by guest on 16 August 2022

was diluted in assay buffer [50 mM HEPES, 20 mM KCl, 5 mM $MgCl_2$, 1 mM DTT, 10 μM ATP (pH 7.4)] and incubated with the peptides. To control for non-proteasomal-mediated cleavage of substrates, a proteasome inhibitor was used in concentrations that give a complete block of the proteasome activity. Values from inhibited samples were subtracted from non-inhibited samples to assess proteasome activity. For the caspase-like and chymotrypsin-like activity, 15 μM and 5 μM epoxomicin were used, respectively and for the trypsin-like activity 40 μM MG132 was used. Samples were incubated with inhibitors at room temperature for 30 min. Activity was assessed by continuous fluorescent measurement of the released AMC at 37°C for 1 h, using a fluorometric plate reader (Varioskan Flash reader). A regression analysis was done on the most linear part of the time/fluorescence curve. The slope of the trend line was taken as a measurement for the proteolytic activity. Littermate Alzheimer's disease and wild-type couples were assayed at the same time. The difference was analysed using paired *t*-tests on couples.

Proteasome constitutive immuno subunit ELISA assay

The proteasome constitutive-immuno subunit ELISA (ProCISE) assay was used to examine the subunit-specific proteasome activities of the constitutive (β5, β1, β2) and immunoproteasome (β5i, β1i, β2i) active sites in tissue samples of mouse cortices from transgenic Alzheimer's Disease and wild-type mice and in hippocampal/entorhinal cortex tissue samples of human donors. This assay was performed as previously described (Parlati *et al*., 2009) with the exception of the use of a different β1 antibody for mouse tissue (Santa Cruz Biotechnology, Catalogue No. sc-67345). Tissue samples were dissolved in lysis buffer (20 mM Tris-HCl pH 8.0, 5 mM EDTA) to 1 mg/ml, then incubated with a proteasome active site probe (5 μM) for 2 h at 25°C. Samples were denatured in 6 M guanidine hydrochloride (Fisher Scientific) and subunits bound to proteasome active site probe were captured with streptavidin-conjugated sepharose beads (GE Healthcare) in 96-well 0.65 μm porous filter plates (Millipore). Individual subunits were probed with subunit-specific primary antibodies, followed by secondary antibodies conjugated to horseradish peroxidase. The SuperSignal ELISA Pico chemiluminescent substrate kit (Pierce) was utilized to generate luminescent signal associated with horseradish peroxidase binding. Luminescence after 5 min of signal development was monitored on a plate reader (Tecan Safire). For mouse samples, subunit activity was expressed as relative luminescence units normalized to protein quantity. For human samples, subunit content was expressed as nanograms of subunit per microgram of total protein, as calculated from a standard curve of human purified constitutive or immunoproteasome, assayed simultaneously with the samples.

Laser dissection microscopy

Sections from snap frozen brains from wild-type and Alzheimer's disease mice of 6, 9 and 12 months were mounted onto glass slides with PENfoil membrane. Slides were washed for 5 min in 70% ethanol and incubated in BTA-1 [2-(4″-(methylamino) phenyl) benzothiazole], diluted in 75% ethanol for 7 min, to visualize amyloid-β plaques. The slides were washed in 70% ethanol, dried and subjected to LMPC. The laser dissection microscopy platform used in this study is the PALM Microbeam system and PALM Software (PALM Robo 3.5). Forty plaques and non-plaque regions were isolated from the somatosensory cortex of Alzheimer's disease and wild-type mice. Dissected areas had a diameter about twice the stained plaque size (Fig. 2A and B). RNA was isolated from the dissected samples as below. Expression was normalized against GAPDH.

Isolation of primary cells for amyloid-β treatment and proteasome inhibition

Ex vivo proteasome inhibition of Alzheimer's disease and wild-type microglia

Alzheimer's disease and wild-type mice were anaesthetized and perfused with Hank's Balanced Salt Solution (−Ca/Mg) (Invitrogen). The cortices were dissected and subjected to mechanical dissociation using Tissue Chopper, followed by enzymatic dissociation using Papain (Worthington) at a final concentration of 8 U/ml together with DNase I at 80 Kunitz units/ml (Sigma) at 37°C for 50 min and thereafter pelleted. The pellet was triturated to single cell suspension in minimal essential media 1% bovine serum albumin and filtered through a 20 μm single cell strainer (BD Biosciences) followed by a separation step over an isotonic (90%) percoll (Amersham Biosciences) at 200*g* for 15 min at 4°C. Top phase was discarded, the other layers were collected and resuspended in minimal essential media 1% bovine serum albumin in five times the volume followed by centrifugation for 10 min at 4°C. Cells were stained with APC labelled CD11b antibody and Fc-receptor block (CD16/32) (all eBioscience), in PBS (0.5% bovine serum albumin) at 4°C for 30 min. The cells were washed and resuspended in PBS/bovine serum albumin and cell viability staining 7AAD (BD bioscience). Using BD FACS Aria I (BD bioscience), CD11b+ microglia were sorted after gating away the dead cell population on 7AAD signal. Sorted microglia were resuspended in Dulbecco's modified Eagle's medium/F-10, 5% foetal bovine serum, 1% penicillin/streptomycin, 20–30 000 cells were inhibited with either 200 nM of the β5i inhibitor ONX-0914 (previously named PR-957) or 125 nM of the PR-825 β5 inhibitor or vehicle for 1 h at 37°C, 5% CO_2. Activity specific concentrations of the inhibitors were based on previous studies (Muchamuel *et al*., 2009; Basler *et al*., 2010). Cells were washed and plated, and stimulated with lipopolysaccharide 1 μg/ml (from *Escherichia coli* 026:B6, L2654, Sigma) for 14 h at 37°C, 5% CO_2. Cells were washed and TRIsure™ was added for RNA isolation (see section below for RNA isolation procedure).

Reverse transcriptase quantitative polymerase chain reaction assays

For gene expression analysis of cortex, the right hemisphere was used for RNA isolation. For human samples 20 times 10 μm sections from snap frozen post-mortem hippocampi obtained from the Netherlands Brain Bank were used (for donor data see Supplementary Table 1). Tissue was homogenized in TRIzol® using an Ultra Turrax. Cells and laser dissection microscopy material were allowed to incubate in TRIzol® for 5 min followed by thorough mixing/vortexing. RNA was isolated by precipitation overnight in isopropanol with addition of 20 μg glycogen. Total RNA was DNaseI treated and used as a template to generate complementary DNA following the manufacturer's instructions (Quantitect-Qiagen). Diluted complementary DNA served as a template in real-time quantitative PCR assays (SYBR® Green PCR Master Mix; Applied Biosystems). Gene expression on mice cortex samples, and isolated microglia samples were normalized using the geometric mean of GAPDH, HPRT and actin expression. Expression levels of human controls and Alzheimer's disease samples were normalized against a selection of 10 reference genes (*GAPDH*, *ACTB*, *PPIA*, *UBE2D2*, *EEF1A*, *RPS27A*, *AARS*, *XPNPEP1*, *RPLP0*, *IPO8*) (Durrenberger *et al*., 2012; Wang

Downloaded from https://academic.oup.com/brain/article/136/5/1415/287013 by guest on 16 August 2022

et al., 2012) based on a geNorm analysis (Vandesompele *et al*., 2002). The normalization factor was the geometric mean of the 10 reference genes. Samples with a RNA integrity (RIN) value <5.0 were excluded from analysis based on a poor correlation with the normalization factor. For primers see Supplementary Table 3.

Statistics

Statistical analyses were done in SPSS, PAWS statistics, 18.0 (Predictive Analytics SoftWare) and GraphPad Prism 5 (GraphPad Software Inc). Data were tested for normal distribution using Shapiro Wilk test for normality. For single comparisons between age-matched Alzheimer's disease and wild-type groups, or between amyloid-β and mock treated samples, significance was tested using a Student's *t*-test or a Mann-Whitney U test. For multiple comparisons between groups the Kruskal-Wallis test with Dunn's multiple comparison was used. For analysis of the human ProCISE assay, an ANOVA was performed using Games-Howell *post hoc* to test for differences between pathology stages. For correlations, Pearson's correlation was used for normally distributed data, in other cases the Spearman's Rho non-parametric correlation was used. In all cases statistical significance was asserted for $P < 0.05$.

Results

Amyloid-β increases the proteasome activity in cultured astrocytes, microglia and neurons

A decrease in proteasome activity has been reported in brain homogenates of patients with Alzheimer's disease (Keller *et al*., 2000; Keck *et al*., 2003; Mishto *et al*., 2006), Alzheimer's disease mouse models (Oh *et al*., 2005; Almeida *et al*., 2006; Tseng *et al*., 2008), and in lysates of amyloid-β treated neurons *in vitro* (Oh *et al*., 2005). Here we investigated the effects of amyloid-$\beta_{1\text{-}42}$ fibrils (fibrillar amyloid-β) and oligomers (oligomeric amyloid-β) on proteasome activity in viable astrocytes, microglia and neuronal cell lines. Cells were treated with 0.1 μM or 1.0 μM of either oligomeric amyloid-β or fibrillar amyloid-β (Supplementary Fig. 1A) for 72 h. The proteasome activity was determined in living cells using a cell-permeable fluorescent proteasome specific probe (Berkers *et al*., 2007; Middeldorp *et al*., 2009) analysed by flow cytometry (Fig. 1A). The probe was shown to be proteasome activity-specific since the fluorescent signal was reduced by adding increasing concentrations of the specific proteasome inhibitor Epoxomicin (Fig. 1B, Supplementary Fig. 1B and C) (Berkers *et al*., 2007). Astrocytes (Fig. 1C), neurons (Fig. 1D), and microglia (Fig. 1E) showed an increased proteasome activity in response to treatment with 1 μM fibrillar amyloid-β or 1 μM oligomeric amyloid-β for 72 h (Fig. 1C–E). In microglia and neurons, fibrillar amyloid-β or oligomeric amyloid-β at a concentration of 0.1 μM had no significant effect on proteasome activity, while 0.1 μM fibrillar amyloid-β increased proteasome activity in astrocytes. In concordance with the results above, astrocytes treated with 1.0 μM fibrillar amyloid-β for 72 h showed enhanced proteolysis of the classical amino-4-methyl coumarin (AMC)-conjugated peptides for chymotrypsin-like and caspase-like activities of the proteasome. Astrocytes treated with oligomeric amyloid-β for 72 h, showed a near significant increase of both peptides (Supplementary Fig. 1D and E). No significant differences in gene expression of constitutive proteasome and immunoproteasome subunits between amyloid-β or mock treated cells were found (Supplementary Fig. 2A and B). To confirm the data from the glial cell lines, mixed primary mouse glial cells were treated with 1.0 μM fibrillar amyloid-β or 1.0 μM oligomeric amyloid-β for 72 h followed by proteasome activity assessment using the cell permeable proteasome activity probe. The proteasome activity of microglia and astrocytes was separated based on positive labelling of the microglia using CD11b + antibodies (see Supplementary Fig 3A–C'' for culture staining and flow cytometry plots). The CD11b − astrocyte population showed a near significant increase in proteasome activity by 15% upon treatment with 1.0 μM fibrillar amyloid-β while no difference was observed with 1.0 μM oligomeric amyloid-β (Fig. 1F and Supplementary Fig. 3C''). The CD11b + microglia population, which made out on average 8.5% of the total cell population, showed a significant 98% increase of proteasome activity upon treatment with 1.0 μM fibrillar amyloid-β, while 1.0 μM oligomeric amyloid-β treatment showed no effect (Fig. 1G and Supplementary Fig. 3C'). Innate immune activation is a reported feature in Alzheimer's disease (Hensley, 2010) and lipopolysaccharide is a potent stimulant of innate immune signalling (Janeway and Medzhitov, 2002). Lipopolysaccharide stimulation of the microglia cell line for 24 h resulted in a 2-fold increase of proteasome activity compared with untreated cells (Fig. 1E), as well as a significant increase in messenger RNA expression of all constitutive proteasome and immunoproteasome proteolytic β-subunits (Fig. 1H). The fold increase of the immunoproteasome subunits was larger than the fold increase of the proteolytic constitutive proteasome subunits (Fig. 1H). Taken together, these data show that especially fibrillar amyloid-β, but also oligomeric amyloid-β increase, rather than inhibit the proteasome activity in living astrocytes, microglia and neurons. Additionally, a strong innate immune activation by lipopolysaccharide elevated the proteasome activity in microglia through increased transcription mainly of the immunoproteasome subunits. These data suggest that in Alzheimer's disease brain proteasome activity may not only be increased as a result of a direct effect of amyloid-β, but also as a consequence of the inflammatory conditions caused by amyloid-β plaque deposition.

Plaque-associated glia show an increase in the expression of immunoproteasome subunits

Several genes involved in ubiquitin proteasome system-mediated protein degradation and markers for glial cell reactivity were analysed by quantitative PCR to determine differential expression in Alzheimer's disease and wild-type mice of different ages. Expression fold changes are shown in Table 1. At 9 months and older, transcript levels of β5i (*Psmb8*) were significantly increased, and from 12 months and older for β1i (*Psmb9*), with the highest fold change of 2.11 for β1i (*Psmb9*) at 18 months and 2.93 for β5i (*Psmb8*) at 12 months (Table 1). No differences were found in transcript levels of the other proteolytic and non-proteolytic β-subunits. Amongst the α-subunits, all but *Psma4*

Downloaded from https://academic.oup.com/brain/article/136/5/1415/287013 by guest on 16 August 2022

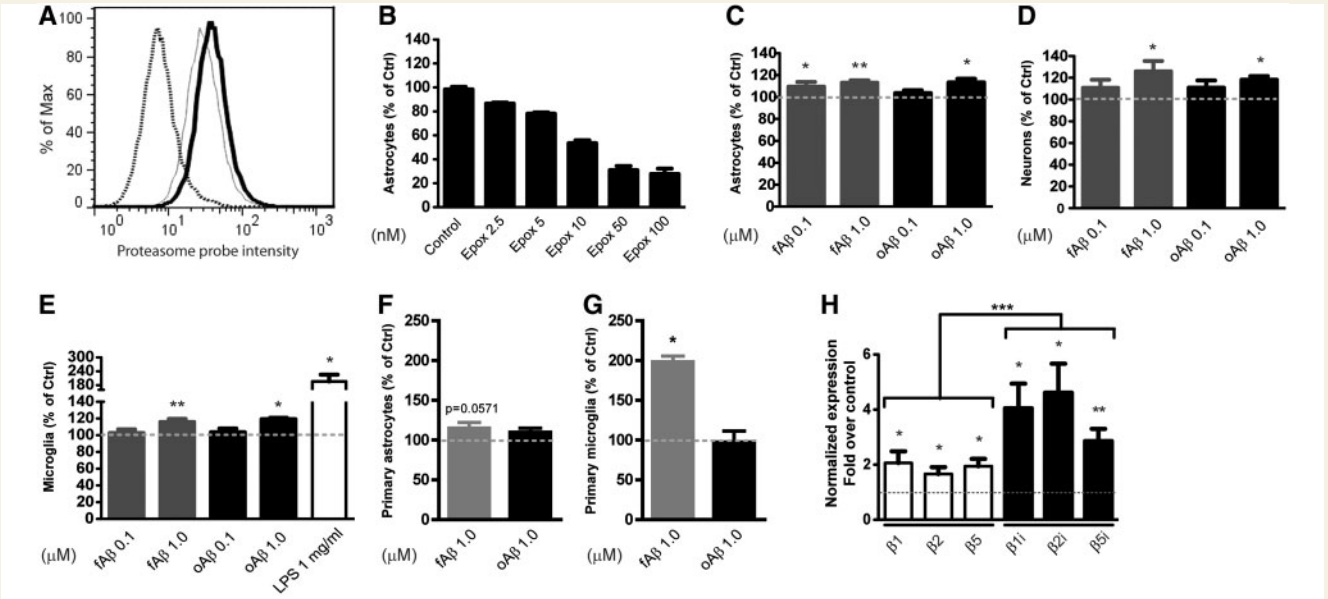

Figure 1 Amyloid-β treatment increases the proteasome activity in living astrocytes, microglia and neurons *in vitro*. (**A**) Histograms showing the fluorescence of the cell-permeable proteasome activity probe as measured by flow cytometry. The *x*-axis shows the probe fluorescence intensity (FL-1). Amyloid-β fibrils (1.0 μM) increased the fluorescence signal, indicating more probe bound and an increase in proteasome activity (solid black line) compared with mock treated controls (solid grey line). Inhibition of the proteasome using Epoxomicin showed strong reduction in fluorescence (dotted black line). (**B**) Treatment with increasing concentrations of the proteasome inhibitor Epoxomicin (2.5–100 nM) for 2 h reduced the fluorescence of the probe in a concentration-dependent manner in Ink4a/Arf$^{-/-}$ astrocytic cells. Proteasome activity measured with the activity probe in (**C**) Ink4a/Arf$^{-/-}$ (astrocytoma), (**D**) N2A (differentiated neuroblastoma), and (**E**) N9 (immortalized microglia) treated with oligomeric amyloid-$\beta_{1\text{-}42}$ and fibrillar amyloid-$\beta_{1\text{-}42}$ in concentrations of 0.1 μM and 1.0 μM for 72 h. (**C–E**) Increased proteasome activity was observed in all three cell types after stimulation with fibrillar amyloid-β (fAβ) and oligomeric amyloid-β (oAβ) at 1.0 μM concentration. Only astrocytes displayed increased proteasome activity to 0.1 μM fibrillar amyloid-β. (**E**) Lipopolysaccharide was used as a positive immune stimulatory control (1 μg/ml) and enhanced the proteasome activity in microglia after 24 h, compared with untreated control. (**F**) Primary astrocytes and (**G**) primary microglia treated with fibrillar amyloid-β and oligomeric amyloid-β at 1.0 μM concentration for 72 h. Primary microglia showed increased proteasome activity after stimulation with 1.0 μM oligomeric amyloid-β compared with mock treated controls (grey dotted line). (**H**) Microglia (N9) stimulated with lipopolysaccharide (1 μg/ml) for 24 h showed an induction of messenger RNA expression of all proteolytic proteasome subunits compared with untreated controls (grey dotted line). The induction of the immunoproteasome expression was higher than the constitutive proteasome expression. (**B–G**) Bars represent average % of proteasome activity compared with mock treated controls from four independent experiments, error bars SEM. Mann-Whitney U test for significance compared with mock treated controls. (**H**) Bars show normalized messenger RNA expression in fold-over untreated control, $n = 6–7$, significance was tested using Mann-Whitney U test. $^*P < 0.05$, $^{**}P < 0.01$.

showed unchanged expression; *Psma4* expression was decreased with 0.63-fold to wild-type at 18 months (Table 1). In the same set of complementary DNA samples, we previously demonstrated increased transcript levels of *Gfap, Cd11b*, and *Cx3cr1* as indicators for reactive gliosis and microglia activation (Kamphuis *et al*., 2012). To obtain evidence that the increase of immunoproteasome transcript levels in Alzheimer's disease mice was associated with amyloid-β plaques, cortical plaque and non-plaque areas were dissected using laser microdissection from brain sections of Alzheimer's disease mice (Fig. 2A and B). Expression levels of immunoproteasome subunits and *Gfap* in microdissected plaque areas were compared with non-plaque areas, and with areas dissected from age-matched wild-type mice (Fig. 2C). Plaque areas showed increased messenger RNA expression levels of β5i (fold change = 11.3) compared with wild-type areas and to Alzheimer's disease non-plaque areas (fold change = 5.0) (Fig. 2C). The expression level of β1i was increased with a fold change of 7.5 compared with wild-type and a fold change of 4.7 compared with non-plaque areas. No change in β2i expression was observed in any of the areas (Fig. 2C). In the same samples *Gfap* levels were significantly increased in plaque areas, which show that the increased expression of immunoproteasome subunits is confined to the astrogliotic area surrounding the amyloid-β plaques.

Immunoproteasome subunits are present in astrocytes and proliferative plaque-associated microglia

To examine whether the increase of transcript levels leads to an increase in protein levels, and to localize the expression to specific cell types, immunostainings for the immunoproteasome subunits were performed in the cortex of Alzheimer's disease mice. Staining for β5i was increased around plaques and overlapped with the microglia-specific marker Iba1 (Fig. 2D–F). In non-activated, ramified microglia, a weak β5i staining was detected that

Downloaded from https://academic.oup.com/brain/article/136/5/1415/287013 by guest on 16 August 2022

Table 1 Expression fold change of proteasome subunits in Alzheimer's disease mice compared with age-matched wild-type mice

	3 months	6 months	9 months	12 months	15 months	18 months
α subunits						
Psma1	1.14 ± 0.18	1.12 ± 0.13	0.91 ± 0.09	1.11 ± 0.21	0.88 ± 0.09	0.77 ± 0.13
Psma2	0.99 ± 0.11	1.15 ± 0.06	1.15 ± 0.17	0.97 ± 0.07	0.93 ± 0.07	0.91 ± 0.06
Psma3	0.67 ± 0.16	1.03 ± 0.12	0.90 ± 0.18	1.10 ± 0.08	0.91 ± 0.15	1.25 ± 0.09
Psma4	0.83 ± 0.08	1.06 ± 0.07	0.88 ± 0.18	0.98 ± 0.08	1.01 ± 0.12	0.63 ± 0.06*
Psma5	1.66 ± 0.51	1.89 ± 0.88	1.38 ± 0.40	1.03 ± 0.20	1.19 ± 0.25	1.26 ± 0.52
Psma6	0.99 ± 0.09	1.24 ± 0.10	0.98 ± 0.15	0.96 ± 0.08	1.11 ± 0.12	0.83 ± 0.09
Psma7	1.60 ± 0.45	0.83 ± 0.25	1.13 ± 0.19	1.24 ± 0.43	0.90 ± 0.34	1.02 ± 0.49
Non-proteolytic β subunits						
Psmb1	1.02 ± 0.11	1.16 ± 0.08	0.86 ± 0.13	1.10 ± 0.11	0.89 ± 0.08	0.91 ± 0.07
Psmb2	1.00 ± 0.08	1.09 ± 0.09	1.19 ± 0.23	0.85 ± 0.15	0.90 ± 0.22	0.76 ± 0.10
Psma3	1.21 ± 0.11	1.04 ± 0.10	0.90 ± 0.17	1.06 ± 0.10	1.00 ± 0.11	0.84 ± 0.06
Psmb4	1.08 ± 0.07	1.08 ± 0.08	1.27 ± 0.23	0.94 ± 0.10	1.04 ± 0.08	0.87 ± 0.04
Proteolytic constitutive β subunits						
Psmb5 (β5)	1.17 ± 0.11	0.99 ± 0.14	1.04 ± 0.14	0.82 ± 0.05	0.95 ± 0.06	1.15 ± 0.13
Psmb6 (β1)	1.34 ± 0.17	1.01 ± 0.10	1.28 ± 0.32	1.11 ± 0.23	0.84 ± 0.10	1.02 ± 0.20
Psmb7 (β2)	0.92 ± 0.11	1.14 ± 0.10	1.12 ± 0.23	1.10 ± 0.11	0.97 ± 0.05	0.78 ± 0.13
Proteolytic immunoproteasome β subunits						
Psmb8 (β5i)	0.79 ± 0.14	1.37 ± 0.20	2.07 ± 0.29*	2.93 ± 0.29**	2.76 ± 0.42***	2.08 ± 0.21**
Psmb9 (β1i)	0.83 ± 0.10	1.00 ± 0.13	1.34 ± 0.24	1.65 ± 0.18**	1.83 ± 0.15***	2.11 ± 0.34**
Psmb10 (β2i)	1.47 ± 0.33	1.09 ± 0.32	1.20 ± 0.23	1.25 ± 0.15	1.23 ± 0.17	1.04 ± 0.35
Proteasome modulators						
Psme1 (PA28α)	1.04 ± 0.08	1.01 ± 0.11	1.20 ± 0.16	1.28 ± 0.15	1.20 ± 0.14	0.90 ± 0.06
Psme4 (PA200)	0.62 ± 0.07	0.95 ± 0.08	1.22 ± 0.26	0.96 ± 0.09	1.10 ± 0.03	0.78 ± 0.11
Psmf1 (Pi31)	1.07 ± 0.12	1.11 ± 0.10	1.57 ± 0.37	0.96 ± 0.08	1.03 ± 0.04	0.97 ± 0.20
Pomp	0.89 ± 0.09	0.99 ± 0.09	1.13 ± 0.13	0.97 ± 0.09	1.01 ± 0.17	0.79 ± 0.07
Glial cell markers						
Gfap	1.58 ± 0.41	2.39 ± 0.70	4.88 ± 1.00***	5.74 ± 0.69***	6.23 ± 0.82***	5.80 ± 0.96***
Itgam (Cd11b)	1.00 ± 0.13	1.31 ± 0.23	2.52 ± 0.82*	1.88 ± 0.25**	2.25 ± 0.25***	1.86 ± 0.28**
Cx3cr1	1.15 ± 0.19	0.95 ± 0.13	2.33 ± 0.67*	2.03 ± 0.28**	2.13 ± 0.10***	1.97 ± 0.30**

Mean fold changes ± SEM of normalized gene expression quantified by reverse transcriptase quantitative PCR. The different proteasome subunits, non-proteolyic α subunits and the proteolytic β subunits, together with astrocyte and microglia markers were analysed and compared between the APPswePS1dE9 Alzheimer's disease mouse and littermate wild-type controls. Significance was tested using Kruskal-Wallis test with Dunn's multiple comparison test, $*P < 0.05$, $**P < 0.001$, $***P < 0.001$. Gene aliases shown in brackets.

was mostly restricted to the nucleus (insert *x* in Fig. 2F), whereas in activated amoeboid microglia, β5i labelling had a more widespread cytosolic distribution (insert *y* in Fig. 2F). A weak nuclear β5i stain was also observed in reactive astrocytes around plaques (Supplementary Fig. 4C and C'). Double staining with earlier injected BrdU (Kamphuis *et al*., 2012) and β5i showed that many β5i+ microglia were proliferating, visualized by BrdU incorporation in cells double positive for β5i and Iba1 (Supplementary Fig. 4D and D'). Increased numbers of β5i and BrdU double positive cells were found in Alzheimer's disease mice (Supplementary Fig. 4E). The expression of β1i was also increased around plaques and co-localized with GFAP (Fig. 2G–I). Some β1i staining showed co-localization with the neuronal marker NeuN (Supplementary Fig. 4A and A''). Immunostaining for β2i displayed a similar staining pattern as for β1i, albeit less clear (Fig. 2J–L; Supplementary Fig. 4B and B'). None of the activated glial cells surrounding plaques showed accumulation of ubiquitin, while dystrophic neurites visualized with an antibody against the C-terminus of amyloid precursor protein were positive for ubiquitin (Supplementary Fig. 5).

Expression of proteasome subunits in Alzheimer's tissue

The immunoproteasome expression in Alzheimer's disease mice was validated in post-mortem tissue from hippocampi of control subjects and patients with Alzheimer's disease. Gene expression levels of the proteolytic immunoproteasome and constitutive proteasome subunits were analysed in hippocampi from control subjects and patients with Alzheimer's disease of different disease stages based on the Braak scores of tau (Braak and Braak, 1991) and amyloid pathology (Thal *et al*., 2000) (see Supplementary Table 1 for clinicopathological information) (Table 2A and B). Expression analysis of the constitutive proteasome subunits showed an overall decrease of β5 (*PSMB5*) expression at all Braak stages reaching statistical significance at Braak 2, 5 and 6 with a 38%, 36% and 38% reduction, respectivly. β5 expression was also reduced when grouping on amyloid score and differed significantly at amyloid score B and C compared with amyloid O by 36% and 35%, respectively. The expression of the other constitutive proteasome subunits did not show significant changes

Downloaded from https://academic.oup.com/brain/article/136/5/1415/287013 by guest on 16 August 2022

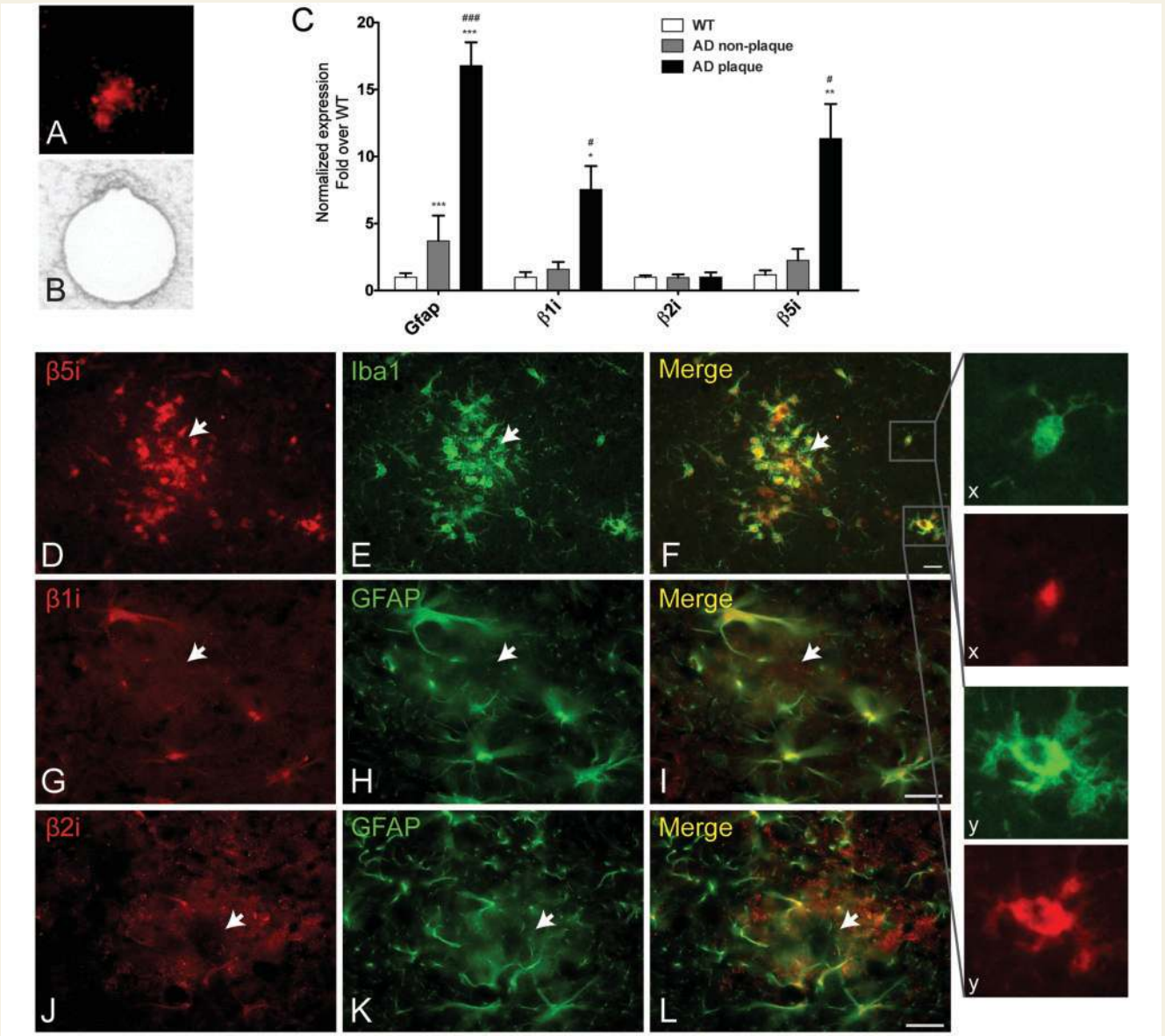

Figure 2 Microglia and astrocytes showed an increase in immunoproteasome expression around amyloid-β plaques in Alzheimer's disease mice. To localize the expression of immunoproteasome and astrocyte reactivity marker, plaque areas stained with BTA-1 were dissected using laser dissection microscopy (**A–B**) together with non-plaque areas from the same tissue and compared with laser dissection microscopy dissected wild-type areas. (**C**) *Gfap* was increased in Alzheimer's disease, both in non-plaque and plaque areas compared with wild-type and in plaque areas compared with non-plaque areas. β1i (*Psmb9*) and β5i (*Psmb8*) expression was upregulated in Alzheimer's disease plaque areas compared with wild-type areas, and in plaque areas compared with non-plaque areas. Expression of *Psmb10* (β2i) showed no differential expression between any of the groups. (**C**) Bars represent normalized messenger RNA expression in fold over wild-type (wild-type: $n = 20$, Alzheimer's disease: $n = 11–12$). *compared with wild-type, #compared with non-plaque. Significance was tested using Mann-Whitney U test, error bars show SEM. ($^{*}P < 0.05$, $^{**}P < 0.01$, $^{***}P < 0.001$; $^{\#}P < 0.5$, $^{\#}P < 0.01$, $^{\#\#\#}P < 0.001$). (**D**) Immunostaining for the immunoproteasome subunit β5i revealed an intense staining around plaques in 9-month-old Alzheimer's disease mice and showed a clear overlap with the Iba1 + microglia (**E**) as shown in the merged picture (**F**). Activated amoeboid shaped microglia showed a more widespread cytosolic β5i staining (insert y) compared with the resting more ramified microglia (insert x). (**G**) Staining for β1i was present in close proximity of plaques and co-localized with GFAP (**H**) as shown in the merged image (**I**). (**J**) β2i immunostaining was found to be only slightly increased around plaques, partly co-localizing with reactive astrocytes (GFAP) (**K** and **L**). Scale bars: **D–L** = 20 μm. Images are representative of at least two independent experiments.

based on either tau or amyloid scores (Table 2A and B). Of the immunoproteasome subunits, the β5i (*PSMB8*) was significantly increased by 42% at Braak 5, compared with the Braak 0 controls, and by 40% at amyloid score C compared with amyloid O. The β2i expression was increased at Braak 2 by 33% compared with Braak 0; no other significant differential immunoproteasome expression was observed (Table 2A and B). Post-mortem delay and sex did not correlate with any constitutive proteasome or immunoproteasome

Downloaded from https://academic.oup.com/brain/article/136/5/1415/287013 by guest on 16 August 2022

Table 2 Changes in expression of proteolytic proteasome subunits in human hippocampus of non-demented control subjects and patients with Alzheimer's disease

A	Braak 1	Braak 2	Braak 3	Braak 4	Braak 5	Braak 6
Proteolytic constitutive β subunits						
PSMB5 (β5)	0.76 ± 0.03	0.62 ± 0.03*	0.68 ± 0.16	0.69 ± 0.08	0.64 ± 0.04*	0.62 ± 0.03**
PSMB6 (β1)	0.90 ± 0.05	0.90 ± 0.07	0.92 ± 0.12	1.05 ± 0.09	0.94 ± 0.05	0.80 ± 0.05
PSMB7 (β2)	0.91 ± 0.06	0.75 ± 0.04	0.95 ± 0.12	0.84 ± 0.03	0.90 ± 0.06	0.75 ± 0.03
Proteolytic immunoproteasome β subunits						
PSMB8 (β5i)	1.21 ± 0.14	0.98 ± 0.10	1.12 ± 0.11	1.29 ± 0.08	1.42 ± 0.08*	1.40 ± 0.26
PSMB9 (β1i)	1.18 ± 0.16	0.90 ± 0.13	0.87 ± 0.08	1.22 ± 0.20	1.17 ± 0.11	1.13 ± 0.19
PSMB10 (β2i)	1.24 ± 0.06	1.67 ± 0.20**	1.42 ± 0.14	1.39 ± 0.14	1.17 ± 0.04	1.05 ± 0.05

B	Amyloid A	Amyloid B	Amyloid C
Proteolytic constitutive β subunits			
PSMB5 (β5)	0.80 ± 0.07	0.64 ± 0.05**	0.65 ± 0.02***
PSMB6 (β1)	0.84 ± 0.11	0.82 ± 0.07	0.84 ± 0.03
PSMB7 (β2)	0.92 ± 0.06	0.79 ± 0.06	0.79 ± 0.03
Proteolytic immunoproteasome β subunits			
PSMB8 (β5i)	1.25 ± 0.18	1.19 ± 0.11	1.40 ± 0.10*
PSMB9 (β1i)	1.30 ± 0.23	1.12 ± 0.13	1.11 ± 0.09
PSMB10 (β2i)	0.93 ± 0.09	1.15 ± 0.08	1.00 ± 0.05

Mean fold changes (compared with Braak 0, or amyloid O controls) ± SEM of normalized gene expression quantified by reverse transcriptase quantitative PCR. The different proteolytic proteasome subunits were compared between tissue showing Alzheimer's disease pathology [based on either (**A**) Tau score (Braak stage) (Braak and Braak, 1991) or (**B**) amyloid score (Thal *et al*., 2000)] and control tissue where no Alzheimer's disease pathology was observed (Braak score 0 or amyloid score O). Donors per Braak stage; $n = 9–23$, and amyloid score; $n = 8–35$. Significance was tested using Kruskal-Wallis test with Dunn's multiple comparison test, $^{*}P < 0.05$, $^{**}P < 0.01$, $^{***}P < 0.001$.

expression. To analyse whether immunoproteasome and constitutive proteasome expression was affected by age, we correlated amyloid O control donors with age and found no significant correlation.

To analyse immunoproteasome protein expression in relation to amyloid-β plaques in human tissue, we performed immunostainings of β1i, β5i and amyloid-β (6E10) on post-mortem tissue of hippocampal / entorhinal cortex from control (Braak 0, Amyloid score O) and Alzheimer's disease tissue (Braak 5, amyloid score C). Despite the amyloid score O, some early amyloid-β plaques were observed in one donor, most of these plaques were surrounded by glial cells with increased immunostaining for β1i (Fig. 3A) and β5i (Fig. 3C), while non-plaque areas showed low β1i and β5i staining. In Alzheimer's disease tissue, the expression of β1i (Fig. 3B and E) and β5i (Fig. 3D and F) was increased throughout the tissue, not only around plaques, but also in areas more distant from plaques. The increased staining was especially confined to cells with glial morphology. Double staining with GFAP showed a large overlap with both β1i and β5i, while the microglia marker, HLA-DR showed some overlap, although to a lesser degree compared with GFAP (Supplementary Figs 6 and 7).

Immunoproteasome activity is increased with increased plaque load in the Alzheimer's disease mouse

Homogenates from cortex of Alzheimer's disease and age-matched wild-type control mice were analysed using an active-site ELISA (Muchamuel *et al*., 2009), allowing an assessment of subunit-specific proteasome activity for the different constitutive proteasome and immunoproteasome subunits. Three groups of Alzheimer's disease animals were analysed, one with low plaque load (3–6 months); intermediate plaque load (9–12 months), and high plaque load (15–18 months) (Kamphuis *et al*., 2012). All three immunoproteasome activities (β5i, β1i, β2i) were significantly elevated in Alzheimer's disease mice compared with their age-matched wild-type groups in the 9–12 month group and the 15–18 month group; β5i (Fig. 4B and C); β1i (Fig. 4E and F) and β2i (Fig. 4H and I). The highest increase was observed in β1i with 272% compared with wild-type littermates at 15–18 months (Fig. 4F). No change in the β5 and β1 activity of the constitutive proteasome was observed (Fig. 4A and D), while the β2 activity was elevated in Alzheimer's disease mice compared with wild-type littermates at 9–12 months and at 15–18 months (Fig. 4G and I). No significant decrease of proteasome activities could be observed in ageing wild-type or Alzheimer's disease mice. Furthermore, an age-dependent, significant increase in β5i, β1i and β2i activity was observed in wild-type mice of 15–18 months of age compared with younger 3–6 month old wild-type mice (Fig. 4B, E and H). The β2 activity was found to be increased in aged wild-type mice of 9–12 and 15–18 months compared with younger wild-type mice of 3–6 months (Fig. 4G).

Additionally, we assessed the proteasome activity with the conventional AMC-peptide hydrolysis method used in previous studies reporting decreased proteasome activity (Keller *et al*., 2000; Keck *et al*., 2003; Oh *et al*., 2005; Almeida *et al*., 2006; Mishto *et al*., 2006; Tseng *et al*., 2008). Cleavage of three commonly used proteasome substrates was analysed to assess caspase-like, chymotrypsin-like, and trypsin-like activity in cortical homogenates of

Downloaded from https://academic.oup.com/brain/article/136/5/1415/287013 by guest on 16 August 2022

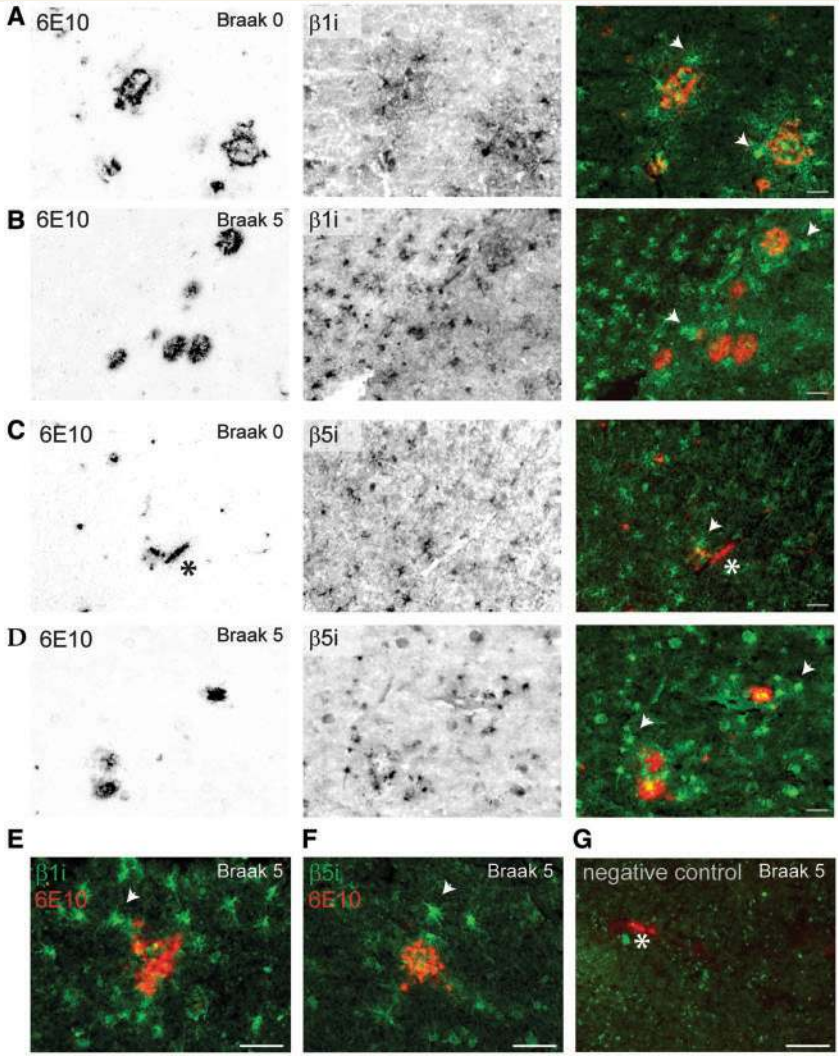

Figure 3 Amyloid-β plaques trigger immunoproteasome expression in reactive glia cells in the human brain. Double staining in the human entorhinal cortex for amyloid-β, using 6E10 monoclonal, and immunoproteasome using β1i and β5i polyclonals, showed that reactive glia (GFAP+ or HLA-DR+, see Supplementary Figs 6 and 7) around amyloid-β+ plaques were positive for immunostaining of the immunoproteasome subunits. (**A–D**) In the first column amyloid-β staining is depicted, in the second column immunoproteasome (β1i or β5i) staining is depicted, and the third column shows merges. Panels **A** and **C** show that the few plaques present in Braak 0 tissue were surrounded by β1i+ and β5i+ glia cells. Panels **B** and **D** show elevated expression of β1i and β5i stain in Alzheimer's disease tissue (Braak 5). Here, a more wide spread glial expression of especially β1i but also β5i was observed, together with a continued high expression of β1i (**E**) and β5i (**F**) in plaque bound glia (Supplementary Figs 6 and 7). (**G**) Negative control with omitted primary antibodies showed no stain, apart for some blood vessel staining in the 'red channel' (alkaline phosphatase) marked by an asterisk. Arrowheads indicate an example of a cell with glial specific morphology. Images represent results from four different donors. Scale bar = 40 μm. Donors: NBB 01-141; 00-107; 01-134.

Alzheimer's disease and wild-type mice of different ages. The caspase-like activity was decreased by 27% in Alzheimer's disease mice at 15 months (Fig. 4J) and the chymotrypsin-like activity was decreased by 17% and 18% at 15 and 18 months, respectively (Fig. 4K) compared with age-matched wild-type mice. The trypsin-like did not differ between Alzheimer's disease and wild-type mice (Fig. 4L). Additionally, no impairment of proteasome activity could be observed when crossing the APPswePS1dE9 mouse with the UbG76VGFP proteasome activity reporter mouse (Supplementary Fig. 8A–C). Thus, the decrease in activity as measured by the AMC peptides assays is likely to be a proteasome-independent effect.

Immunoproteasome activity is increased in human Alzheimer's disease samples

A total of 64 human control and Alzheimer's disease post-mortem hippocampal tissue samples were selected based on tau and amyloid scores and analysed for subunit specific constitutive

Downloaded from https://academic.oup.com/brain/article/136/5/1415/287013 by guest on 16 August 2022

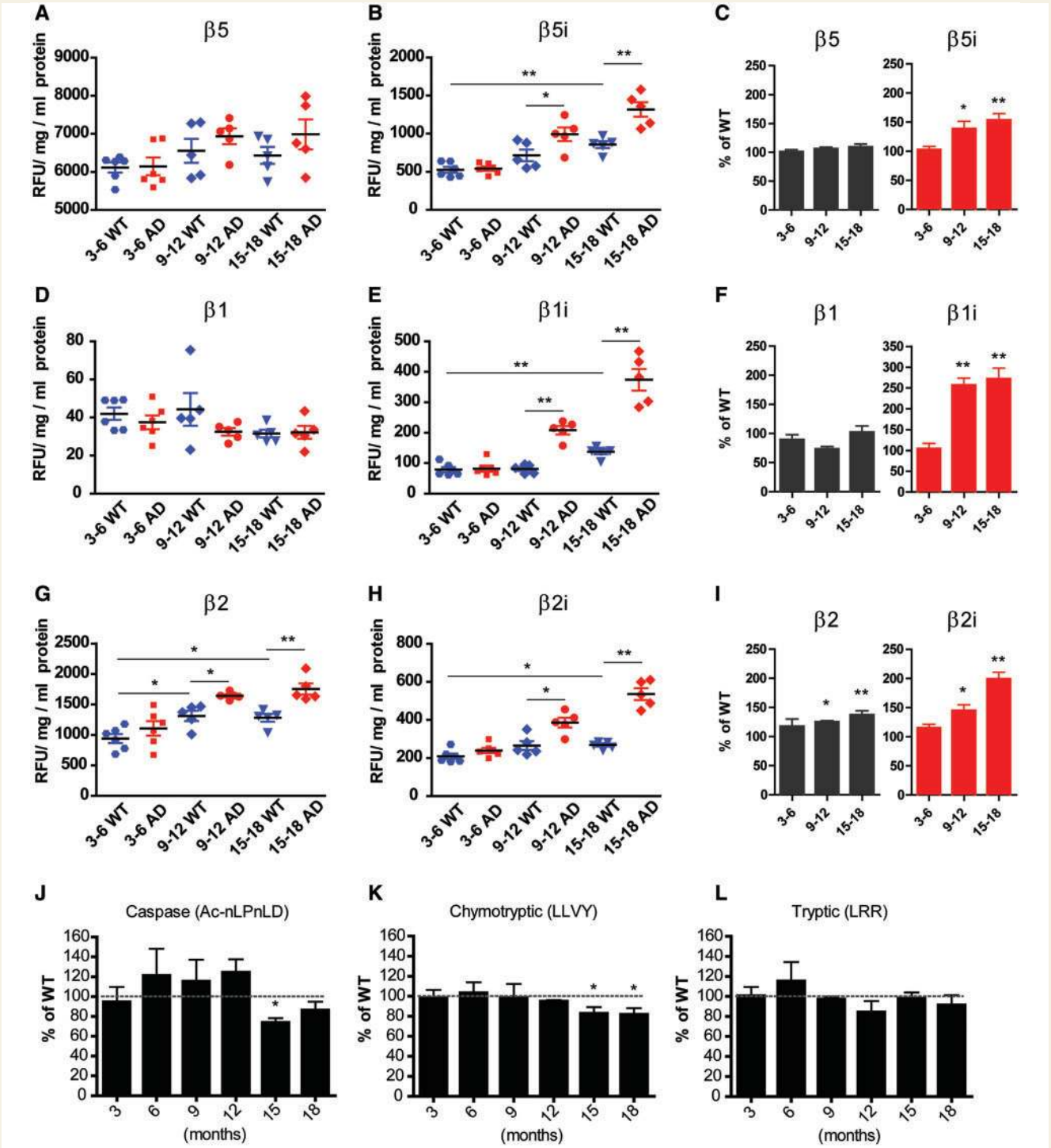

Figure 4 The immunoproteasome activity is increased with age and plaque load in Alzheimer's disease mice. Proteasome activity in cortex of Alzheimer's disease and wild-type mice was measured with an activity ELISA (ProCISE) (**A–I**) and peptide hydrolysis assays (**J–L**). Proteasome activity of constitutive proteasome and immunoproteasome subunits measured in homogenates of APPswePS1dE9 and wild-type mice of different ages. **A**, **D** and **G** show constitutive proteasome activities and **B**, **E** and **H** show immunoproteasome activities in relative fluorescent unit (RFU)/protein concentration. Change in activity is shown as % of age-matched wild-type in (**C**, **F** and **I**). No change in constitutive proteasome β5 activity (**A** and **C**) or β1 activity (**D** and **F**) was observed between Alzheimer's disease and wild-type mice in any of the age groups. The β2 constitutive proteasome activity was increased in Alzheimer's disease mice compared with wild-type mice at 9–12 months and at 15–18 months and in aged wild-type mice compared with younger wild-type mice (**G** and **I**). All three immunoproteasome activities were increased in Alzheimer's disease mice compared with age-matched wild-type mice. The β5i activity (**B** and **C**); the β1i activity (**E** and **F**) and the β2i activity (**H** and **I**) were increased in Alzheimer's disease at 9–12 months and at 15–18 months. All three immunoproteasome activities were increased in aged wild-type mice compared with younger wild-type mice (**B**, **E** and **H**).

(continued)

Downloaded from https://academic.oup.com/brain/article/136/5/1415/287013 by guest on 16 August 2022

proteasome and immunoproteasome activity, as previously done in the mouse samples. When grouping samples on Braak tau scores, no difference in any of the constitutive proteasome activities was observed between the different Braak stages (Fig. 5A–C). In contrast, the three immunoproteasome activities were elevated with increased tau pathology; the β1i activity was increased by 82% at Braak 4 compared with Braak 0 controls (Fig. 5D). The β2i activity was increased at Braak 4, 5 and 6 groups compared with the Braak 0 controls with largest increase of 59% at Braak 5; the Braak 6 group also differed significantly from the Braak 1 group (Fig. 5E). The β5i activity was significantly increased in Braak 4, and 6 compared with Braak 0, with the highest increase of 62% at Braak 6 (Fig. 5F).

When grouping the samples based on amyloid scores, the amyloid scores A and B did not differ significantly and were pooled due to their low sample numbers. The β2 activity was increased by

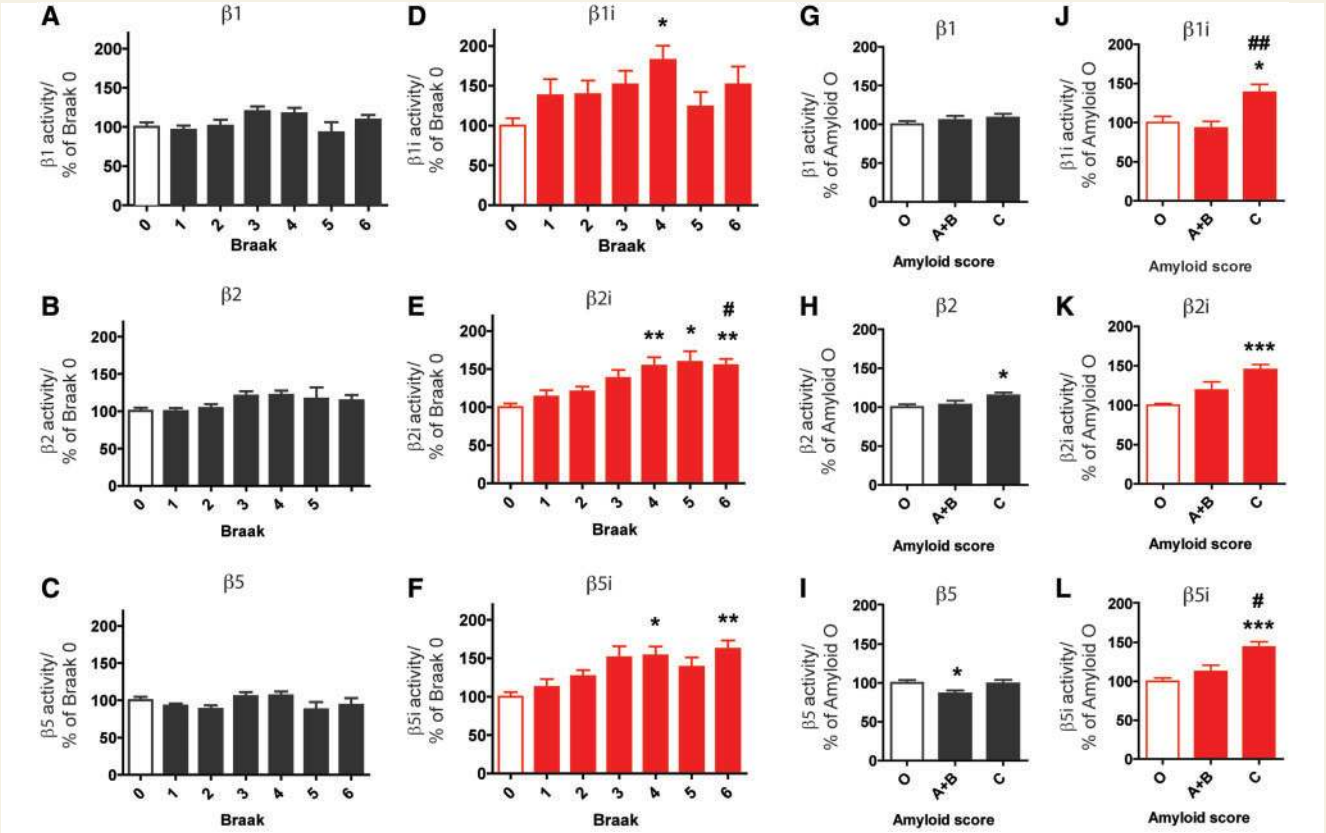

Figure 5 The immunoproteasome activity is increased with Alzheimer's disease pathology in human post-mortem tissue. Proteasome activity of constitutive proteasome and immunoproteasome subunits was assessed in human post-mortem hippocampal/entorhinal cortex tissue from control subjects and Alzheimer's disease donors using the ProCISE assay. (**A–C**) The constitutive proteasome activities grouped on Braak (tau) staging. (**G–I**) The constitutive proteasome activities grouped on amyloid score, amyloid score A and B were pooled in this analysis. (**J–L**) The different immunoproteasome activities grouped on amyloid score; all three subunits showed increased activity in the amyloid C group compared with O. Bars show mean of subunit activity in % of controls (Braak 0 or amyloid O), error bars show SEM, $n = 9–12$ per Braak stage and $n = 14–28$ per amyloid score. Significance was tested with ANOVA using Games-Howell *post hoc* correction, $^{*}P < 0.05$, $^{**}P < 0.01$, $^{***}P < 0.001$ compared with Braak 0 or amyloid O controls, $^{\#}P < 0.05$, $^{\#\#}P < 0.01$ compared with Braak 1 or amyloid A + B.

Figure 4 Continued

(**J–L**) The proteasome activity measured in the same homogenates using the peptide hydrolysis method, using activity specific AMC-conjugated probes. (**J**) Caspase activity showed impaired activity at 15 months. (**K**) Chymotryptic activity was decreased in 15 and 18 month Alzheimer's disease mice. (**L**) The trypsin-like measured did not show any significant changes between wild-type and Alzheimer's disease. (**A**, **B**, **D**, **E**, **G** and **H**) The *y*-axis indicates relative fluorescent units normalized on protein load, black lines mark the group mean, error bars show SEM. (**C**, **F** and **I**) The *y*-axis shows activity in % of age matched wild-type, the bars show the group mean, error bars show SEM, $n = 5–6$. Significance was tested using Mann-Whitney U test. (**J–L**) Bars show mean of proteolytic activity in % of wild-type littermate controls, error bars show SEM, $n = 8–9$ and significance was tested using Students paired *t*-test on Alzheimer's disease and wild-type littermate couples assayed at the same time. $^{*}P < 0.05$, $^{**}P < 0.01$, $^{***}P < 0.001$.

Downloaded from https://academic.oup.com/brain/article/136/5/1415/287013 by guest on 16 August 2022

15% in amyloid score C compared with amyloid O controls (Fig. 5H), while the β5 activity showed a transient impairment of 14% in the amyloid A + B, but remained unchanged at amyloid C compared with amyloid O (Fig. 5I). All immunoproteasome activities (β5i, β1i, β2i) were significantly higher in the amyloid C group compared with O group (44%; 39%; 46%, respectively). The β1i and β5i activities were also increased compared with the amyloid A + B group (Fig. 5J–L). After correcting for age, using a partial correlation analysis, all the immunoproteasome activities showed a positive correlation for amyloid score, the β5i and β2i activities significant while the β1i activity showed a near significant correlation [Pearsons' r: β5i, 0.536 ($P < 0.0001$); β2i, 0.543 ($P < 0.0001$) and β1i, 0.283 ($P = 0.054$)]; for Braak tau score the β5i and β2i activities showed a positive significant correlation [Pearsons' r: β5i, 0.554 ($P < 0.001$); β2i, 0.630 ($P < 0.001$)]. No significant correlation between the activity of the constitutive proteasome subunits and tau or amyloid score was observed.

Inhibition of β5i activity reduced pro-inflammatory signalling in microglia isolated from Alzheimer's disease and wild-type mice

As shown in Fig. 1E, stimulation with lipopolysaccharide increased proteasome activity in microglia. lipopolysaccharide acts through the CD14 receptor to induce innate immune signalling (Jiang *et al*., 2005). CD14 and TLR2 are also amyloid-β recognition receptors, involved in amyloid-β induced activation of innate immune signalling (Liu *et al*., 2005, 2012). To investigate whether CD14 and TLR2 were implicated in the plaque pathology of this Alzheimer's disease mouse model, we analysed their gene expression in the cortex. Elevated levels of both *Cd14* and *Tlr2* transcripts were observed in Alzheimer's disease compared with wild-type mice after the emergence of plaques, starting from 9 months and onward (Fig. 6A and B). Previously, inhibition of β5i immunoproteasome activity reduced innate pro-inflammatory signalling in peripheral immune cells (Muchamuel *et al*., 2009). We hypothesized that an inhibition of the elevated β5i activity in Alzheimer's disease microglia would lead to a decrease in pro-inflammatory signalling. Therefore, microglia from 15 month-old Alzheimer's disease and wild-type mice were acutely isolated and treated *ex vivo* with specific β5 or β5i inhibitors [as used in previous studies (Muchamuel *et al*., 2009; Basler *et al*., 2010)]. Inhibition was followed by lipopolysaccharide stimulation to further stimulate the CD14-mediated signalling pathways (Fig. 6C). Very low or undetectable levels of *Cd14*, *Tnf* and *Il1b* was observed in non-lipopolysaccharide stimulated Alzheimer's disease or wild-type microglia (Fig. 6D, F and G). Firstly, upon lipopolysaccharide stimulation, we observed that microglia from Alzheimer's disease mice showed higher messenger RNA expression of *Cd14*, *Tlr2* and *Il1b* compared with wild-type microglia (Fig. 6D, E and G). Secondly, inhibition of the enhanced β5i activity using ONX 0914 led to a significant attenuation of *Cd14, Tlr2* and *Il1b* expression in response to lipopolysaccharide stimulation (Fig. 6D, E and H). Thirdly, *Tnf* messenger RNA expression was equally elevated after lipopolysaccharide stimulation in both Alzheimer's disease and wild-type microglia. Here, inhibition of β5i activity caused a significant reduction of lipopolysaccharide-induced *Tnf* expression in both groups (Fig. 6F). In most cases, inhibition of the constitutive β5 activity using PR-825 led to a slight, but non-significant, reduction of gene expression compared with vehicle control (Fig. 6D–F). These data accentuate the strong involvement of the immunoproteasome, especially the β5i subunit in regulating the elevated innate immune signalling observed in this Alzheimer's disease mouse model.

Discussion

The present study reports in detail, for the first time, on the activity of all proteasome subunits in an Alzheimer's disease mouse model and in human post-mortem brain tissue of non-demented control subjects and patients at different stages of Alzheimer's disease. We reveal a clear increase of immunoproteasome activity in both the Alzheimer's disease mouse and in human Alzheimer's disease tissue using a novel and highly sensitive method to assess subunit-specific proteasome activity. The transcript levels of the immunoproteasome subunits were also elevated in mice with a higher plaque-load, but remained mainly unregulated in the human Alzheimer's disease tissue, in contrast with their corresponding activity. Moreover, we found no impairment of activity in any of the immunoproteasome or constitutive proteasome subunits in the Alzheimer's disease mouse and in human Alzheimer's disease pathology, apart from a slight transient impairment of the β5 activity, at amyloid score A + B in the human tissue. Our findings are in contrast with the impairment of proteasome activity observed in all earlier studies in brain homogenates of human Alzheimer's disease and mouse Alzheimer's disease brain samples (Keller *et al*., 2000; Keck *et al*., 2003; Oh *et al*., 2005; Almeida *et al*., 2006; Mishto *et al*., 2006; Tseng *et al*., 2008). Together with accumulation of ubiquitinated proteins in Alzheimer's disease brains, this led to the widely held belief that proteasome inhibition is a prominent feature of Alzheimer's disease pathology (Fergusson *et al*., 1996). Here we show that ubiquitin accumulation is confined to dystrophic neurites around plaques in the Alzheimer's disease mouse, and not present in glia. However, because we do not observe any reduction in immunoproteasome or constitutive proteasome activity, we argue that the accumulation of dystrophic neurites is not due to a decreased proteasome activity. The previous proteasome activity studies were all based on hydrolysis of AMC-conjugated peptides; therefore we also used this method here, to assess proteasome activity, along with the subunit-specific activity-ELISA. Using the AMC peptides, we found a slight decrease in chymotrypsin-like and caspase-like proteasome activity in older Alzheimer's disease mice. Though this finding is in line with previous studies, it is in contrast with the results of the activity-ELISA assay. The discrepancy between the two methods is likely to be due to several limitations of the AMC peptide hydrolysis assays. One problem is its relative aspecificity (Rodgers and Dean, 2003), as the AMC substrates can also be cleaved by other proteases, like calpains and caspases (Kisselev and Goldberg, 2005). Furthermore, the AMC peptides cannot distinguish

Downloaded from https://academic.oup.com/brain/article/136/5/1415/287013 by guest on 16 August 2022

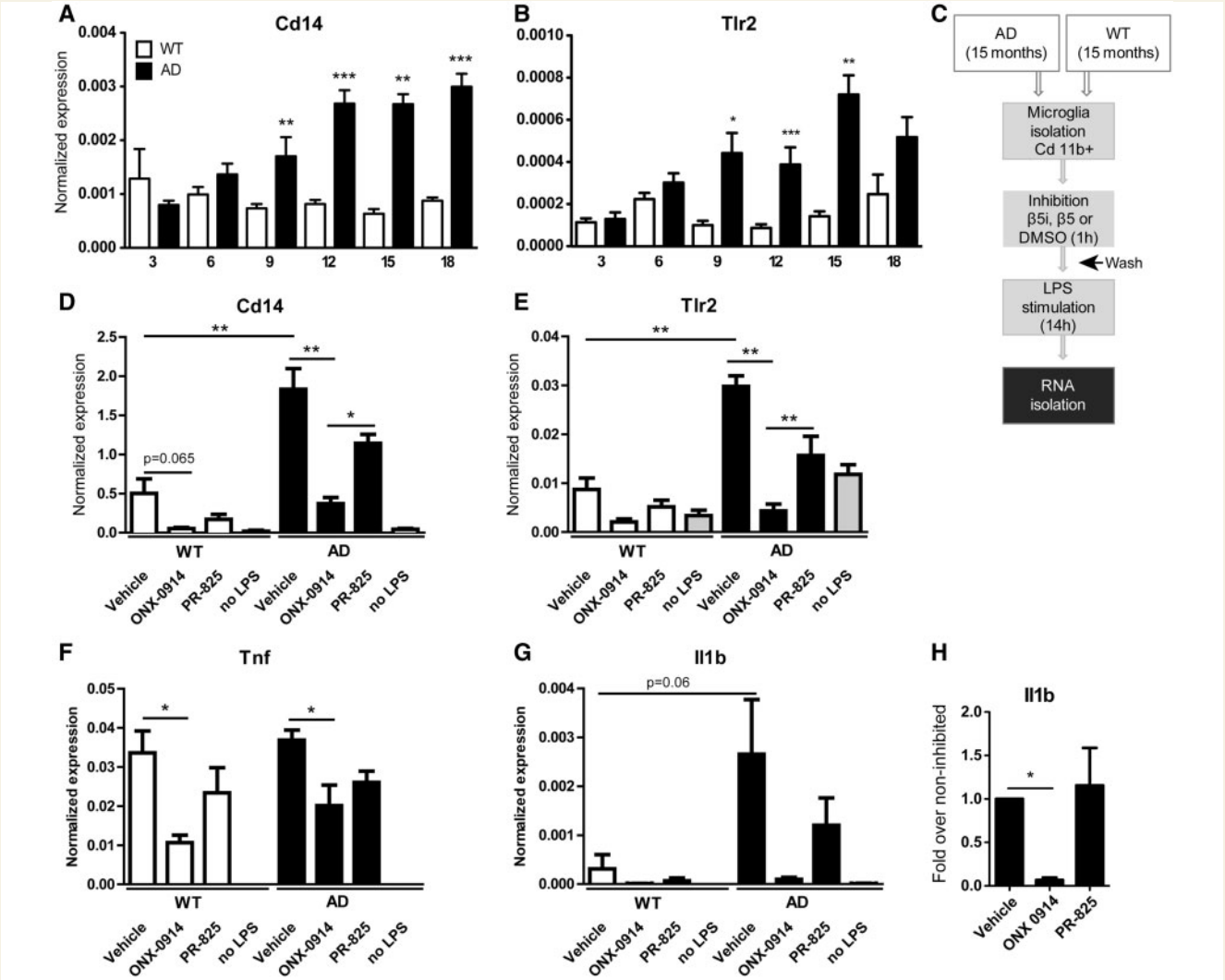

Figure 6 Specific inhibition of the immunoproteasome β5i activity reduced pro-inflammatory signalling in microglia isolated from aged Alzheimer's disease and wild-type mice. (**A–B**) The receptors CD14 and TLR2 have been implicated in recognition of amyloid-β and activation of innate immune signalling. The levels of *Cd14* and *Tlr2* were elevated in cortex of Alzheimer's disease mice compared with wild-type mice, starting from 9 months (n = 6–9), bars show normalized messenger RNA expression. (**C**) Schematic overview of inhibition and stimulation scheme of isolated microglia from 15 month-old Alzheimer's disease and wild-type mice. β5i and β5 activity was inhibited using specific inhibitors (ONX 0914 for β5i, PR-825 for β5), prior lipopolysaccharide (LPS) stimulation of isolated Alzheimer's disease and wild-type microglia. (**D–E**) *Cd14* and *Tlr2* expression were higher in Alzheimer's disease microglia compared to wild-type microglia after lipopolysaccharide stimulation. Inhibition of β5i activity prevented the lipopolysaccharide induced *Cd14* and *Tlr2* expression in Alzheimer's disease microglia to similar levels as of the non-lipopolysaccharide stimulated microglia. (**F**) No difference in induction of *Tnf* expression was observed between Alzheimer's disease and wild-type microglia. Here, β5i inhibition reduced the *Tnf* levels in both groups. (**G**) *Il1b* expression was low in wild-type microglia, undetectable in a few samples. Microglia isolated from Alzheimer's disease mice showed increased expression of *Il1b* after lipopolysaccharide stimulation; which was strongly reduced in the β5i-inhibited samples (**H**) compared with vehicle treated samples. In all cases, inhibition of β5 had no significant effect on the expression of these genes. (**D–G**) Bars show normalized gene expression, error bars show SEM, n = 5 (no lipopolysaccharide n = 2), significance tested using Mann-Whitney U test. (**H**) Bars show fold over vehicle control, error bars SEM, significance tested using one sample t-test. DMSO = dimethyl sulphoxide.

between constitutive proteasome and immunoproteasome subunit activity (Kisselev and Goldberg, 2005; Ferrington *et al*., 2008), while the activity-ELISA assay is able to do so.

In contrast with the previously published proteasome activity data, protein levels of the immunoproteasome were reported to be elevated in Alzheimer's disease brains by western blot and immunohistochemistry (Mishto *et al*., 2006; Nijholt *et al*., 2011). Also in other diseases with strong reactive gliosis, such as multiple sclerosis (Mishto *et al*., 2010), AIDS dementia (Nguyen *et al*., 2009), and epilepsy (Mishto *et al*., 2011), increased immunoproteasome levels were found. It has been suggested that the induction of immunoproteasome could 'hijack' the function of the constitutive proteasome, leading to a dysfunction of the latter (Nguyen *et al*., 2009). However, such an effect cannot be

Downloaded from https://academic.oup.com/brain/article/136/5/1415/287013 by guest on 16 August 2022

confirmed here, since the upregulation of immunoproteasome activities did not coincide with a significant impairment of the constitutive proteasome activities in either the Alzheimer's disease mice or in the human Alzheimer's disease tissue.

Using the same model as in our study, Aso *et al*. (2011) found elevated protein levels of β1i and β2i, together with a reduction in the chymotrypsin-like activity in aged Alzheimer's disease mice. This led the authors to argue that the immunoproteasome was dysfunctional. An increased expression of immunoproteasome has also been observed in chronically inflamed tissues such as inflammatory bowel disease (Schmidt *et al*., 2010) and chronic hepatitis (French *et al*., 2011), the latter concomitant with sustained Toll-like receptor activity. Here we showed an increase in immunoproteasome activity together with an increased immunoproteasome staining of glia around plaques in Alzheimer's disease tissue (mouse and human). In the Alzheimer's disease mouse we also demonstrate that this upregulation is confined to plaques by analysing microdissected plaque and non-plaque areas. In addition, we show that cell cultures treated with amyloid-β show increased proteasome activity, especially primary microglia. All of these observations indicate that amyloid-β deposition underlies the increased immunoproteasome expression, most likely in response to an amyloid-β-induced TLR/CD14 receptor activation (Liu *et al*., 2005; Reed-Geaghan *et al*., 2009; Cameron *et al*., 2012) as discussed below. To further prove that TLR/CD14 signalling can bring about increased immunoproteasome expression and proteasome activity, we stimulated microglia with lipopolysaccharide and observed a strong induction of predominantly immunoproteasome subunits, and an increased proteasome activity.

The immunoproteasome is known to have a role in pro-inflammatory cytokine regulation involved in the innate immune response, believed to be mediated by NF-κB transcription, although the exact mechanism is not completely known (Groettrup *et al*., 2010; Hensley *et al*., 2010). An increased proteasome activity and elevated immunoproteasome levels has previously been shown upon IFNγ stimulation (Gaczynska *et al*., 1993), and in mouse brains after a cytotoxic T cell injury, where increased immunoproteasome expression in microglia, astrocytes, and oligodendrocytes was observed (Ferrington *et al*., 2008). Amyloid-β-induced activation of NF-κB has been shown in astrocytes (Wang *et al*., 2010) and in microglia (Delgado *et al*., 2008). The increase of immunoproteasome activity observed, together with elevated pro-inflammatory signalling in Alzheimer's disease mice (Hickman *et al*., 2008; Ruan *et al*., 2009; Kamphuis *et al*., 2012), is likely to be a response to an activation of the innate immune response by amyloid-β. This process might be mediated by CD14, which has been shown to be involved in amyloid-β recognition in microglia cells (Liu *et al*., 2005). We show that *Cd14* expression is elevated in relation to plaque load. Taken together, these data suggest that the reactive glia cells surrounding plaques may have entered a long-lasting, pro-inflammatory state, with increased immunoproteasome expression and activity, likely through sustained TLR2/CD14-dependent signalling. This may have detrimental effects on the homeostatic functioning of astrocytes (Henn *et al*., 2011) and is likely to contribute to neuronal excitotoxicity (Verkhratsky and Parpura, 2010). Introduction of a CD14 null mutation in the APPswePS1dE9 line, led to a reduction of plaque load, implicating that a reduction of CD14 levels is beneficial for plaque clearance (Reed-Geaghan *et al*., 2010). Additionally, a deletion of TLR2 in monocytes and microglia reduced cytokine release and improved amyloid-β phagocytosis (Liu *et al*., 2012). While Alzheimer's disease mice with a global TLR2 deficiency showed impaired memory and elevated amyloid-β levels (Richard *et al*., 2008). An initial activation of the innate immune response may be beneficial for amyloid-β clearance (DiCarlo, 2001), therefore increased immunoproteasome levels may be beneficial to enhance the degradation of oxidized and damaged proteins that accumulate under acute inflammatory cell stress (Pickering *et al*., 2010; Seifert *et al*., 2010). However, a sustained dysregulation of immune signalling is a known feature of Alzheimer's disease and is likely to be a key contributor in the pathophysiology of Alzheimer's disease (as reviewed in Heneka *et al*., 2010). Sustained immune signalling has previously been shown to lead to reduced levels of amyloid-β recognition receptors and of amyloid-β degrading enzymes in microglia from aged Alzheimer's disease mice (Hickman *et al*., 2008), as well as a reduction of general cognitive functions (Corona *et al*., 2011). A continuously elevated immunoproteasome activity may be accountable for the sustained innate immune response, which in turn contributes to glial dysfunction and increased oxidative stress. A mild inhibition of the proteasome attenuated tissue damage and had antioxidative effects in a rat model of diabetic nephropathy (Luo *et al*., 2011). Specific inhibition of the β5i activity reduces levels of pro-inflammatory molecules and tissue damage in a rheumatoid arthritis mouse model and in a model of inflammatory bowel disease (Muchamuel *et al*., 2009; Basler *et al*., 2010). Moreover, lipopolysaccharide stimulation of macrophages isolated from LMP7/MECL1 (β5i/β2i) knockout mice was associated with suppression of cytokine secretion (Reis *et al*., 2011). Here we show that inhibition of the elevated β5i activity, for the first time in brain cells, leads to a reduction of several innate immune signalling molecules and receptors. These results clearly indicate that β5i inhibitors possess anti-inflammatory properties.

This study provides a paradigm shifting view on the function of the ubiquitin proteasome system in relation to plaque pathology in Alzheimer's disease, and points to its involvement in neuroinflammation and its association with glial reactivity. To target the elevated β5i activity with a β5i specific inhibitor, *in vivo*, would be a potential strategy to reduce the sustained pro-inflammatory signalling in Alzheimer's disease, without affecting other essential functions of the ubiquitin proteasome system. Additional studies to further investigate this novel interaction between immunoproteasome, amyloid-β induced glial reactivity, and neuroinflammation, are needed to fully elucidate their relationship in Alzheimer's disease.

Acknowledgements

We thank D. Borchelt for the APPswePS1dE9 mouse and the Netherlands Brain Bank for human brain tissue, W. Scheper, L. de Kimpe and R. Zwart for help with making Aβ preparations. We also thank S. Copray for the N9 cell line, and M. van Lohuizen for the Ink/Arf$^{-/-}$, N. Dantuma for the UbG76VGFP

Downloaded from https://academic.oup.com/brain/article/136/5/1415/287013 by guest on 16 August 2022

reporter mouse, A. Alkemade for lipopolysaccharide, and I. Klaassen for proteasome antibodies.

Funding

This work was supported by the Internationale Stichting Alzheimer Onderzoek [ISAO 08504], NANONET COST [BM1002], and the Netherlands Organization for Scientific Research [NWO; VICI grant 865.09.003 to E.M.H.].

Conflict of interest

Christopher J. Kirk and Elena T. Chan are employees and stockholders of Onyx Pharmaceuticals.

Supplementary material

Supplementary material is available at *Brain* online.

References

Almeida CG, Takahashi RH, Gouras GK. Beta-amyloid accumulation impairs multivesicular body sorting by inhibiting the ubiquitin-proteasome system. J Neurosci 2006; 26: 4277–4288.

Aso E, Lomoio S, Lopez-Gonzalez I, Joda L, Carmona M, Fernandez-Yague N, et al. Amyloid generation and dysfunctional immunoproteasome activation with disease progression in animal model of familial Alzheimer disease. Brain Pathol 2011; 22: 636–53.

Basler M, Dajee M, Moll C, Groettrup M, Kirk CJ. Prevention of experimental colitis by a selective inhibitor of the immunoproteasome. J Immunol 2010; 185: 634–41.

Beach TG, Walker R, McGeer EG. Patterns of gliosis in Alzheimer's disease and aging cerebrum. Glia 1989; 2: 420–36.

Berkers CR, Van Leeuwen FWB, Groothuis TA, Peperzak V, Van Tilburg EW, Borst J, et al. Profiling proteasome activity in tissue with fluorescent probes. Mol Pharm 2007; 4: 739–48.

Braak H, Braak E. Neuropathological stageing of Alzheimer-related changes. Acta Neuropathol 1991; 82: 239–59.

Cameron B, Tse W, Lamb R, Li X, Lamb BT, Landreth GE. Loss of interleukin receptor-associated kinase 4 signaling suppresses amyloid pathology and alters microglial phenotype in a mouse model of Alzheimer's disease. J Neurosci 2012; 32: 15112–23.

Chafekar SM, Hoozemans JJ, Zwart R, Baas F, Scheper W. Abeta 1-42 induces mild endoplasmic reticulum stress in an aggregation state-dependent manner. Antioxid Redox Signal 2007; 9: 2245–54.

Corona AW, Fenn AM, Godbout JP. Cognitive and behavioral consequences of impaired immunoregulation in aging. J Neuroimmune Pharmacol 2011; 7: 7–23.

Delgado M, Varela N, Gonzalez-Rey E. Vasoactive intestinal peptide protects against beta-amyloid-induced neurodegeneration by inhibiting microglia activation at multiple levels. Glia 2008; 56: 1091–103.

DiCarlo G, Wilcock D, Henderson D, Gordon M, Morgan D. Intrahippocampal LPS injections reduce Aβ load in APP + PS1 transgenic mice. Neurobiol Aging 2001; 22: 1007–012.

Durrenberger PF, Fernando FS, Magliozzi R, Kashefi SN, Bonnert TP, Ferrer I, et al. Selection of novel reference genes for use in the human central nervous system: a BrainNet Europe Study. Acta Neuropathol 2012; 124: 893–903.

Fergusson J, Landon M, Lowe J, Dawson SP, Layfield R, Hanger DP, et al. Pathological lesions of Alzheimer's disease and dementia with Lewy bodies brains exhibit immunoreactivity to an ATPase that is a regulatory subunit of the 26S proteasome. Neurosci Lett 1996; 219: 167–70.

Ferrington DA, Hussong SA, Roehrich H, Kapphahn RJ, Kavanaugh SM, Heuss ND, et al. Immunoproteasome responds to injury in the retina and brain. J Neurochem 2008; 106: 158–69.

French BA, Oliva J, Bardag-Gorce F, French SW. The immunoproteasome in steatohepatitis: its role in Mallory–Denk body formation. Exp Mol Pathol 2011; 90: 252–6.

Früh K, Gossen M, Wang K, Bujard H, Peterson PA, Yang Y. Displacement of housekeeping proteasome subunits by MHC-encoded LMPs: a newly discovered mechanism for modulating the multicatalytic proteinase complex. EMBO J 1994; 13: 3236–44.

Gaczynska M, Rock KL, Goldberg AL. Gamma-interferon and expression of MHC genes regulate peptide hydrolysis by proteasomes. Nature 1993; 365: 264–7.

Goldberg AL. Protein degradation and protection against misfolded or damaged proteins. Nature 2003; 426: 895–9.

Groettrup M, Kirk CJ, Basler M. Proteasomes in immune cells: more than peptide producers? Nat Rev Immunol 2010; 10: 73–8.

Heneka MT, O'Banion MK, Terwel D, Kummer MP. Neuroinflammatory processes in Alzheimer's disease. J Neural Transm 2010; 117: 919–47.

Henn A, Kirner S, Leist M. TLR2 Hypersensitivity of astrocytes as functional consequence of previous inflammatory episodes. J Immunol 2011; 186: 3237–47.

Hensley K. Neuroinflammation in Alzheimer's disease: mechanisms, pathologic consequences, and potential for therapeutic manipulation. J Alzheimers Dis 2010; 21: 1–14.

Hensley SE, Zanker D, Dolan BP, David A, Hickman HD, Embry AC, et al. Unexpected role for the immunoproteasome subunit LMP2 in antiviral humoral and innate immune responses. J Immunol 2010; 184: 4115–22.

Hickman SE, Allison EK, El Khoury J. Microglial dysfunction and defective beta-amyloid clearance pathways in aging Alzheimer's disease mice. J Neurosci 2008; 28: 8354–60.

Janeway CA Jr, Medzhitov R. Innate immune recognition. Annu Rev Immunol 2002; 20: 197–216.

Jankowsky JL, Slunt HH, Gonzales V, Jenkins NA, Copeland NG, Borchelt DR. APP processing and amyloid deposition in mice haploinsufficient for presenilin 1. Neurobiol Aging 2004; 25: 885–92.

Jiang Z, Georgel P, Du X, Shamel L, Sovath S, Mudd S, et al. CD14 is required for MyD88-independent LPS signaling. Nat Immunol 2005; 6: 565–70.

Kamphuis W, Orre M, Kooijman L, Dahmen M, Hol EM. Differential cell proliferation in the cortex of the APPswePS1dE9 Alzheimer's disease mouse model. Glia 2012; 60: 615–29.

Keck S, Nitsch R, Grune T, Ullrich O. Proteasome inhibition by paired helical filament-tau in brains of patients with Alzheimer's disease. J Neurochem 2003; 85: 115–22.

Keller JN, Hanni KB, Markesbery WR. Impaired proteasome function in Alzheimer's disease. J Neurochem 2000; 75: 436–9.

Kincaid EZ, Che JW, York I, Escobar H, Reyes-Vargas E, Delgado JC, et al. Mice completely lacking immunoproteasomes show major changes in antigen presentation. Nat Immunol 2011; 13: 129–35.

Kisselev AF, Goldberg AL. Monitoring activity and inhibition of 26S proteasomes with fluorogenic peptide substrates. Methods Enzymol 2005; 398: 364–78.

Lindsten K, Menendez-Benito V, Masucci MG, Dantuma NP. A transgenic mouse model of the ubiquitin/proteasome system. Nat Biotechnol 2003; 21: 897–902.

Liu S, Liu Yang, Hao W, Wolf L, Kiliaan AJ, Penke B, et al. TLR2 Is a Primary receptor for Alzheimer's amyloid β peptide to trigger neuroinflammatory activation. J Immunol 2012; 188: 1098–107.

Liu Y, Walter S, Stagi M, Cherny D, Letiembre M, Schulz-Schaeffer W, et al. LPS receptor (CD14): a receptor for phagocytosis of Alzheimer's amyloid peptide. Brain 2005; 128: 1778–89.

Luo ZF, Qi W, Feng B, Mu J, Zeng W, Guo YH, et al. Prevention of diabetic nephropathy in rats through enhanced renal

Downloaded from https://academic.oup.com/brain/article/136/5/1415/287013 by guest on 16 August 2022

antioxidative capacity by inhibition of the proteasome. Life Sci 2011; 88: 512–20.
Mamber C, Kamphuis W, Haring NL, Peprah N, Middeldorp J, Hol EM. GFAPδ Expression in glia of the developmental and adolescent mouse brain. PLoS One 2012; 7: e52659.
Middeldorp J, Kamphuis W, Sluijs JA, Achoui D, Leenaars CH, Feenstra MG, et al. Intermediate filament transcription in astrocytes is repressed by proteasome inhibition. FASEB J 2009; 23: 2710–26.
Mishto M, Bellavista E, Ligorio C, Textoris-Taube K, Santoro A, Giordano M, et al. Immunoproteasome LMP2 60HH variant alters MBP epitope generation and reduces the risk to develop multiple sclerosis in Italian female population. PLoS One 2010; 5: e9287.
Mishto M, Bellavista E, Santoro A, Stolzing A, Ligorio C, Nacmias B, et al. Immunoproteasome and LMP2 polymorphism in aged and Alzheimer's disease brains. Neurobiol Aging 2006; 27: 54–66.
Mishto M, Ligorio C, Bellavista E, Martucci M, Santoro A, Giulioni M, et al. Immunoproteasome expression is induced in mesial temporal lobe epilepsy. Biochem Biophys Res Commun 2011; 408: 65–70.
Muchamuel T, Basler M, Aujay MA, Suzuki E, Kalim KW, Lauer C, et al. A selective inhibitor of the immunoproteasome subunit LMP7 blocks cytokine production and attenuates progression of experimental arthritis. Nat. Med. 2009; 15: 781–7.
Nguyen TP, Soukup VM, Gelman BB. Persistent hijacking of brain proteasomes in HIV-associated dementia. Am J Pathol 2009; 176: 893–902.
Nijholt DA, De Graaf TR, Van Haastert ES, Oliveira AO, Berkers CR, Zwart R, et al. Endoplasmic reticulum stress activates autophagy but not the proteasome in neuronal cells: implications for Alzheimer's disease. Cell Death Differ 2011; 18: 1071–81.
Oh S, Hong HS, Hwang E, Sim HJ, Lee W, Shin SJ, et al. Amyloid peptide attenuates the proteasome activity in neuronal cells. Mech Ageing Dev 2005; 126: 1292–9.
Palombella VJ, Rando OJ, Goldberg AL, Maniatis T. The ubiquitin-proteasome pathway is required for processing the NF-kappa B1 precursor protein and the activation of NF-kappa B. Cell 1994; 78: 773–85.
Parlati F, Lee SJ, Aujay M, Suzuki E, Levitsky K, Lorens JB, et al. Carfilzomib can induce tumor cell death through selective inhibition of the chymotrypsin-like activity of the proteasome. Blood 2009; 114: 3439–47.
Perry VH, Nicoll JA, Holmes C. Microglia in neurodegenerative disease. Nat Rev Neurol 2010; 6: 193–201.
Pickering AM, Koop AL, Teoh CY, Ermak G, Grune T, Davies KJ. The immunoproteasome, the 20S proteasome and the PA28alphabeta proteasome regulator are oxidative-stress-adaptive proteolytic complexes. Biochem J 2010; 432: 585–94.
Reed-Geaghan EG, Reed QW, Cramer PE, Landreth GE. Deletion of CD14 attenuates AD pathology by influencing the brain's inflammatory milieu. J Neurosci 2010; 30: 15369–73.
Reed-Geaghan EG, Savage JC, Hise AG, Landreth GE. CD14 and toll-like receptors 2 and 4 are required for fibrillar A{beta}-stimulated microglial activation. J Neurosci 2009; 29: 11982–92.
Reis J, Hassan F, Guan XQ, Shen J, Monaco JJ, Papasian CJ, et al. The immunoproteasomes regulate LPS-induced TRIF/TRAM signaling pathway in murine macrophages. Cell Biochem Biophys 2011; 60: 119–26.
Richard KL, Filali M, Préfontaine P, Rivest S. Toll-like receptor 2 acts as a natural innate immune receptor to clear Amyloid β_{1-42} and delay the cognitive decline in a mouse model of Alzheimer's disease. J Neurosci 2008; 28: 5784–93.
Rodgers KJ, Dean RT. Assessment of proteasome activity in cell lysates and tissue homogenates using peptide substrates. Int J Biochem Cell Biol 2003; 35: 716–27.
Ruan L, Kang Z, Pei G, Le Y. Amyloid deposition and inflammation in Appswe/Ps1de9 mouse model of Alzheimer's disease. Curr Alzheimer Res 2009; 6: 531–40.
Schmidt N, Gonzalez E, Visekruna A, Kühl AA, Loddenkemper C, Mollenkopf H, et al. Targeting the proteasome: partial inhibition of the proteasome by bortezomib or deletion of the immunosubunit LMP7 attenuates experimental colitis. Gut 2010; 59: 896–906.
Schubert D, Soucek T, Blouw B. The induction of HIF-1 reduces astrocyte activation by amyloid beta peptide. Eur J Neurosci 2009; 29: 1323–34.
Seifert U, Bialy LP, Ebstein F, Bech-Otschir D, Voigt A, Schroter F, et al. Immunoproteasomes preserve protein homeostasis upon interferon-induced oxidative stress. Cell 2010; 142: 613–24.
Selkoe DJ. Alzheimer's disease: genes, proteins, and therapy. Physiol Rev 2001; 81: 741–66.
Thal DR, Rüb U, Schultz C, Sassin I, Ghebremedhin E, Del Tredici K, et al. Sequence of Abeta-protein deposition in the human medial temporal lobe. J Neuropathol Exp Neurol 2000; 59: 733–48.
Tseng BP, Green KN, Chan JL, Blurton-Jones M, LaFerla FM. Abeta inhibits the proteasome and enhances amyloid and tau accumulation. Neurobiol Aging 2008; 29: 1607–18.
Vandesompele J, De Preter K, Pattyn F, Poppe B, Van Roy N, DePaepe A, et al. Accurate normalization of real-time quantitative RT-PCR data by geometric averaging of multiple interval control genes. Genome Biol 2002; 3: 0034.1–0034.11.
Verkhratsky A, Parpura V. Recent advances in (patho)physiology of astroglia. Acta Pharmacol Sin 2010; 31: 1044–54.
De Vrij FM, Fischer DF, Van Leeuwen FW, Hol EM. Protein quality control in Alzheimer's disease by the ubiquitin proteasome system. Prog Neurobiol 2004; 74: 249–70.
Wang HM, Zhao YX, Zhang S, Liu GD, Kang WY, Tang HD, et al. PPARgamma agonist curcumin reduces the amyloid-beta-stimulated inflammatory responses in primary astrocytes. J Alzheimers Dis 2010; 20: 1189–99.
Wang Q, Ishikawa T, Michiue T, Zhu BL, Guan DW, Maeda H. Stability of endogenous reference genes in postmortem human brains for normalization of quantitative real-time PCR data: comprehensive evaluation using geNorm, NormFinder, and BestKeeper. Int J Legal Med 2012; 126: 943–52.

Downloaded from https://academic.oup.com/brain/article/136/5/1415/287013 by guest on 16 August 2022